rounds of the viral genome replication per S phase in CIN612-9E cells, and that forced expression of E1 in W12 cells converted HPV16 DNA replication to random-choice replication (12). Interestingly, when HPV16 or HPV31 DNAs are separately introduced into NIKS cells, they both replicate randomly (12). Thus, it is likely that the difference between W12 and CIN612-9E cells depends on expression levels of E1. It is possible that occasional or low-level expression of auxiliary E1 hinders the copy number loss for an even longer period of maintenance, as indicated by previous studies (18, 39). Theoretically, E1 protein could be supplied from the infected virion and/or by *de novo* synthesis from the infected viral genome in the establishment stage. In this regard, it is not clear whether our experimental system recapitulates the actual establishment stage of the HPV life cycle, since E1 can be supplied only by *de novo* synthesis. At present, little is known about the underlying mechanisms of the establishment stage and the mechanism(s) of switching to the subsequent maintenance stage. Clearly, it needs to be examined whether the E1 protein is included in infectious virions and how the E1 expression is regulated in the three different stages.

PV E1 protein forms double hexamers at the replication origin in the LCR with the help of E2 (2, 11, 43) and unwinds DNA through helicase activity ahead of replication forks powered by the hydrolysis of ATP (31). Since E1 is the only viral protein with enzymatic activities, it is an attractive target for development of novel therapeutic agents to treat HPV-associated benign lesions where the whole viral life cycle is completed. Indeed, some candidate small molecules have been reported to inhibit the E1 function (5, 9, 15, 40–42). However, their identification and evaluation was done using biochemical assays or surrogate cell-based assays, and a true antiviral activity has yet to be tested. Based on our present study, the effectiveness of E1 inhibitors as antiviral drugs may be restricted, since they cannot inhibit E1-independent HPV replication in long-living basal cells. Inhibition of E1 protein function could prevent amplification of the viral genome in the establishment and productive stages. Thus, it may prevent HPV infection and reduce pathogenesis, including papilloma formation and virion production. In the case of cervical intraepithelial neoplasias (CINs), continuous inhibition of E1 might reverse low-grade lesions to apparently healthy mucosa, but interruption of the inhibition might lead to recurrence of the lesions. More importantly, it may not be able to eliminate the HPV genomes replicating in undifferentiated basal cells, which are thought to be the histogenetic origin of cervical cancer. Thus, E1 inhibition might not be able to prevent CIN lesions from progressing into cancer.

In summary, we have established an experimental system which can evaluate the requirement of any viral gene of interest in the viral life cycle by supplying and deleting exogenous expression of the gene and demonstrated that E1 is entirely dispensable for maintenance replication of the HPV16 genome in human keratinocytes. Thus, inhibition of E1 may not be able to eliminate the viral genome from the basal cell layer. The rationale for development of E1 inhibitors as anti-HPV drugs may be more restricted than formerly envisaged. Further studies will be required to elucidate the roles of cellular replication factors and the *cis* elements of the HPV genome in E1-independent maintenance replication.

ACKNOWLEDGMENTS

We express our appreciation to Takako Ishiyama for expert technical assistance. We are grateful to John H. Lee (University of Iowa Hospitals and Clinics) for the loxP-HPV16-loxP construct, Izumu Saito (University of Tokyo and RIKEN RDB) for adenovirus vectors, and Hiroyuki Miyoshi (RIKEN BRC) for lentivirus vectors and packaging constructs.

This work was supported in part by Grants-in-Aid for Cancer Research from the Ministry of Health Labor and Welfare to T.K., and for Scientific Research from the Ministry of Education, Culture, Sports, Science, and Technology of Japan to N.E., T.N., and T.K.

REFERENCES

1. **Angeletti PC, Kim K, Fernandes FJ, Lambert PF.** 2002. Stable replication of papillomavirus genomes in *Saccharomyces cerevisiae*. J. Virol. **76**:3350–3358.
2. **Berg M, Stenlund A.** 1997. Functional interactions between papillomavirus E1 and E2 proteins. J. Virol. **71**:3853–3863.
3. **Buchholz F, Angrand PO, Stewart AF.** 1998. Improved properties of FLP recombinase evolved by cycling mutagenesis. Nat. Biotechnol. **16**:657–662.
4. **Chiang CM, et al.** 1992. Viral E1 and E2 proteins support replication of homologous and heterologous papillomaviral origins. Proc. Natl. Acad. Sci. U. S. A. **89**:5799–5803.
5. **D'Abramo CM, Archambault J.** 2011. Small molecule inhibitors of human papillomavirus protein-protein interactions. Open Virol. J. **5**:80–95.
6. **Del Vecchio AM, Romanczuk H, Howley PM, Baker CC.** 1992. Transient replication of human papillomavirus DNAs. J. Virol. **66**:5949–5958.
7. **Doorbar J.** 2006. Molecular biology of human papillomavirus infection and cervical cancer. Clin. Sci. (Lond.) **110**:525–541.
8. **Egawa K.** 2003. Do human papillomaviruses target epidermal stem cells? Dermatology **207**:251–254.
9. **Faucher AM, et al.** 2004. Discovery of small-molecule inhibitors of the ATPase activity of human papillomavirus E1 helicase. J. Med. Chem. **47**:18–21.
10. **Fradet-Turcotte A, et al.** 2011. Nuclear accumulation of the papillomavirus E1 helicase blocks S-phase progression and triggers an ATM-dependent DNA damage response. J. Virol. **85**:8996–9012.
11. **Frattini MG, Laimins LA.** 1994. Binding of the human papillomavirus E1 origin-recognition protein is regulated through complex formation with the E2 enhancer-binding protein. Proc. Natl. Acad. Sci. U. S. A. **91**:12398–12402.
12. **Hoffmann R, Hirt B, Bechtold V, Beard P, Raj K.** 2006. Different modes of human papillomavirus DNA replication during maintenance. J. Virol. **80**:4431–4439.
13. **Jeon S, Lambert PF.** 1995. Integration of human papillomavirus type 16 DNA into the human genome leads to increased stability of E6 and E7 mRNAs: implications for cervical carcinogenesis. Proc. Natl. Acad. Sci. U. S. A. **92**:1654–1658.
14. **Kanegae Y, et al.** 1996. Efficient gene activation system on mammalian cell chromosomes using recombinant adenovirus producing Cre recombinase. Gene **181**:207–212.
15. **Kasukawa H, Howley PM, Benson JD.** 1998. A fifteen-amino-acid peptide inhibits human papillomavirus E1–E2 interaction and human papillomavirus DNA replication in vitro. J. Virol. **72**:8166–8173.
16. **Kim K, Angeletti PC, Hassebroek EC, Lambert PF.** 2005. Identification of *cis*-acting elements that mediate the replication and maintenance of human papillomavirus type 16 genomes in *Saccharomyces cerevisiae*. J. Virol. **79**:5933–5942.
17. **Kim K, Lambert PF.** 2002. E1 protein of bovine papillomavirus 1 is not required for the maintenance of viral plasmid DNA replication. Virology **293**:10–14.
18. **Lee JH, et al.** 2004. Propagation of infectious human papillomavirus type 16 by using an adenovirus and Cre/LoxP mechanism. Proc. Natl. Acad. Sci. U. S. A. **101**:2094–2099.
19. **Lindner SE, Sugden B.** 2007. The plasmid replicon of Epstein-Barr virus: mechanistic insights into efficient, licensed, extrachromosomal replication in human cells. Plasmid **58**:1–12.
20. **Lu JZ, Sun YN, Rose RC, Bonnez W, McCance DJ.** 1993. Two E2 binding sites (E2BS) alone or one E2BS plus an A/T-rich region are minimal requirements for the replication of the human papillomavirus type 11 origin. J. Virol. **67**:7131–7139.
21. **Maglennon GA, McIntosh P, Doorbar J.** 2011. Persistence of viral DNA in the epithelial basal layer suggests a model for papillomavirus latency following immune regression. Virology **414**:153–163.

22. **Maiorano D, Lemaitre JM, Mechali M.** 2000. Stepwise regulated chromatin assembly of MCM2-7 proteins. J. Biol. Chem. **275**:8426–8431.
23. **Mungal S, Steinberg BM, Taichman LB.** 1992. Replication of plasmid-derived human papillomavirus type 11 DNA in cultured keratinocytes. J. Virol. **66**:3220–3224.
24. **Nakano M, Ishimura M, Chiba J, Kanegae Y, Saito I.** 2001. DNA substrates influence the recombination efficiency mediated by FLP recombinase expressed in mammalian cells. Microbiol. Immunol. **45**:657–665.
25. **Nanbo A, Sugden A, Sugden B.** 2007. The coupling of synthesis and partitioning of EBV's plasmid replicon is revealed in live cells. EMBO J. **26**:4252–4262.
26. **Narisawa-Saito M, et al.** 2007. HPV16 E6-mediated stabilization of ErbB2 in neoplastic transformation of human cervical keratinocytes. Oncogene **26**:2988–2996.
27. **Naviaux RK, Costanzi E, Haas M, Verma IM.** 1996. The pCL vector system: rapid production of helper-free, high-titer, recombinant retroviruses. J. Virol. **70**:5701–5705.
28. **Pittayakhajonwut D, Angeletti PC.** 2008. Analysis of *cis*-elements that facilitate extrachromosomal persistence of human papillomavirus genomes. Virology **374**:304–314.
29. **Pittayakhajonwut D, Angeletti PC.** 2010. Viral *trans*-factor independent replication of human papillomavirus genomes. Virol. J. **7**:123.
30. **Rabson MS, Yee C, Yang YC, Howley PM.** 1986. Bovine papillomavirus type 1 3′ early region transformation and plasmid maintenance functions. J. Virol. **60**:626–634.
31. **Rocque WJ, et al.** 2000. Replication-associated activities of purified human papillomavirus type 11 E1 helicase. Protein Expr. Purif. **18**:148–159.
32. **Sakakibara N, Mitra R, McBride A.** 2011. The papillomavirus E1 helicase activates a cellular DNA damage response in viral replication foci. J. Virol. **85**:8981–8995.
33. **Sasaki R, et al.** 2009. Oncogenic transformation of human ovarian surface epithelial cells with defined cellular oncogenes. Carcinogenesis **30**:423–431.
34. **Schmitt A, et al.** 1996. The primary target cells of the high-risk cottontail rabbit papillomavirus colocalize with hair follicle stem cells. J. Virol. **70**: 1912–1922.
35. **Sverdrup F, Khan SA.** 1994. Replication of human papillomavirus (HPV) DNAs supported by the HPV type 18 E1 and E2 proteins. J. Virol. **68**:505–509.
36. **Takata Y, Kondo S, Goda N, Kanegae Y, Saito I.** 2011. Comparison of efficiency between FLPe and Cre for recombinase-mediated cassette exchange in vitro and in adenovirus vector production. Genes Cells **16**:765–777.
37. **Ustav M, Stenlund A.** 1991. Transient replication of BPV-1 requires two viral polypeptides encoded by the E1 and E2 open reading frames. EMBO J. **10**:449–457.
38. **Ustav M, Ustav E, Szymanski P, Stenlund A.** 1991. Identification of the origin of replication of bovine papillomavirus and characterization of the viral origin recognition factor E1. EMBO J. **10**:4321–4329.
39. **Wang HK, Duffy AA, Broker TR, Chow LT.** 2009. Robust production and passaging of infectious HPV in squamous epithelium of primary human keratinocytes. Genes Dev. **23**:181–194.
40. **White PW, Faucher AM, Goudreau N.** 2011. Small molecule inhibitors of the human papillomavirus E1-E2 interaction. Curr. Top. Microbiol. Immunol. **348**:61–88.
41. **White PW, et al.** 2005. Biphenylsulfonacetic acid inhibitors of the human papillomavirus type 6 E1 helicase inhibit ATP hydrolysis by an allosteric mechanism involving tyrosine 486. Antimicrob. Agents Chemother. **49**: 4834–4842.
42. **White PW, et al.** 2003. Inhibition of human papillomavirus DNA replication by small molecule antagonists of the E1-E2 protein interaction. J. Biol. Chem. **278**:26765–26772.
43. **Yang L, Li R, Mohr IJ, Clark R, Botchan MR.** 1991. Activation of BPV-1 replication in vitro by the transcription factor E2. Nature **353**:628–632.
44. **Yates JL, Guan N.** 1991. Epstein-Barr virus-derived plasmids replicate only once per cell cycle and are not amplified after entry into cells. J. Virol. **65**:483–488.
45. **zur Hausen H.** 2002. Papillomaviruses and cancer: from basic studies to clinical application. Nat. Rev. Cancer **2**:342–350.

OPEN ACCESS Freely available online

PLoS one

Establishment of Functioning Human Corneal Endothelial Cell Line with High Growth Potential

Tadashi Yokoi[1,2], Yuko Seko[1,7], Tae Yokoi[1], Hatsune Makino[3], Shin Hatou[4], Masakazu Yamada[5], Tohru Kiyono[6], Akihiro Umezawa[3], Hiroshi Nishina[2], Noriyuki Azuma[1]*

1 Department of Ophthalomology, National Center for Child Health and Development, Tokyo, Japan, **2** Department of Developmental and Regenerative Biology, Medical Research Institute, Tokyo Medical and Dental University, Bunkyo-ku Tokyo, Japan, **3** Department of Reproductive Biology, National Research Institute for Child Health and Development, Tokyo, Japan, **4** Department of Ophthalmology, Keio University School of Medicine, Tokyo, Japan, **5** Division for Vision Research, National Institute of Sensory Organs, National Tokyo Medical Center, Tokyo, Japan, **6** Division of Virology, National Cancer Center Research Institute, Tokyo, Japan, **7** Sensory Functions Section, Research Institute, National Rehabilitation Center for Persons with Disabilities, Tokyo, Japan

Abstract

Hexagonal-shaped human corneal endothelial cells (HCEC) form a monolayer by adhering tightly through their intercellular adhesion molecules. Located at the posterior corneal surface, they maintain corneal translucency by dehydrating the corneal stroma, mainly through the Na^+- and K^+-dependent ATPase (Na^+/K^+-ATPase). Because HCEC proliferative activity is low *in vivo*, once HCEC are damaged and their numbers decrease, the cornea begins to show opacity due to overhydration, resulting in loss of vision. HCEC cell cycle arrest occurs at the G1 phase and is partly regulated by cyclin-dependent kinase inhibitors (CKIs) in the Rb pathway (p16-CDK4/CyclinD1-pRb). In this study, we tried to activate proliferation of HCEC by inhibiting CKIs. Retroviral transduction was used to generate two new HCEC lines: transduced human corneal endothelial cell by human papillomavirus type E6/E7 (THCEC (E6/E7)) and transduced human corneal endothelial cell by Cdk4R24C/CyclinD1 (THCEH (Cyclin)). Reverse transcriptase polymerase chain reaction analysis of gene expression revealed little difference between THCEC (E6/E7), THCEH (Cyclin) and non-transduced HCEC, but cell cycle-related genes were up-regulated in THCEC (E6/E7) and THCEH (Cyclin). THCEH (Cyclin) expressed intercellular molecules including ZO-1 and N-cadherin and showed similar Na^+/K^+-ATPase pump function to HCEC, which was not demonstrated in THCEC (E6/E7). This study shows that HCEC cell cycle activation can be achieved by inhibiting CKIs even while maintaining critical pump function and morphology.

Citation: Yokoi T, Seko Y, Yokoi T, Makino H, Hatou S, et al. (2012) Establishment of Functioning Human Corneal Endothelial Cell Line with High Growth Potential. PLoS ONE 7(1): e29677. doi:10.1371/journal.pone.0029677

Editor: Irina Kerkis, Instituto Butantan, Brazil

Received July 18, 2011; **Accepted** December 2, 2011; **Published** January 19, 2012

Funding: This study was supported by a grant (#18390473) from the Ministry of Education, Culture, Sports, Science and Technology (MEXT) of Japan. The funders had no role in study design, data collection and analysis, decision to publish, or preparation of the manuscript.

Competing Interests: The authors have declared that no competing interests exist.

* E-mail: azuma-n@ncchd.go.jp

Introduction

Human corneal endothelial cells (HCEC) are hexagonal in shape and form a fragile monolayer lying posterior to the surface of the cornea. These cells maintain corneal transparency by their tight intercellular barrier and perform an ion transport pump function through Na^+/K^+-ATPase, which regulates the hydration of the corneal stroma [1,2]. If HCEC sustain damage, excessive hydration and opacity of the cornea occur, resulting in decreased vision.

Corneal endothelia are believed not to increase in adult humans and in fact gradually decrease by approximately 0.5% per year [3,4,5]. Damage, injury or HCEC disease such as Fuchs' corneal dystrophy [6], diabetes [7], trauma [8], cataract surgery [9] or elevation of intraocular pressure [10] does not lead to increased proliferation but rather to an increase in cell size to compensate for the wounded area [11]. Once the cell number falls below 1,000 cells/mm^2, the monolayer of enlarged HCEC cannot maintain corneal translucency [12] and surgical treatment is required to restore vision.

Penetrating keratoplasty has long been the surgical treatment of choice, involving replacement of a total layer of cornea by donor material. However, it can also result in adverse effects such as astigmatism and severe rejection requiring long term usage of immunosuppressive drugs [13]. Recently, alternative transplantation strategies, including modified posterior lamellar keratoplasty techniques such as deep lamellar endothelial keratoplasty (DLEK) [14], Descemet's stripping with endothelial keratoplasty (DSEK) [15] and Descemet membrane endothelial keratoplasty (DMEK) [16] have been introduced to overcome these problems. Despite these advances, an increasingly aging population requiring corneal transplants and inadequate tissue quality limit the availability of donor corneas, such that alternative ways of preparing endothelial cell monolayers need to be explored.

HCEC were originally believed to be incapable of expanding *in vitro*, but have been successfully isolated and cultured by introducing stimulating agents such as epidermal growth factor, platelet-derived growth factor-BB, bovine pituitary extract and fetal bovine serum [17,18]. However, the number of cells with proliferative activity and the ability to respond to such agents is relatively low, and much variation in proliferative activity exists between donors of different ages [19,20]. Thus, there is a requirement to achieve a stable and effective culture of cells in terms of both cell proliferation and physiologic function.

The HCEC cell cycle is mainly regulated by the p53 and pRB pathways, both of which have been inactivated by human papilloma virus (HPV) type 16 E6/E7 to successfully immortalize cells. Kim et al. reported the establishment of an immortalized HCEC line using HPV type 16 E6/E7 on lyophilized human amniotic membrane [21]. However, several studies have reported carcinogenesis of the cell line established by viral oncogenes including HPV type 16 E6/E7 or SV40 large T antigen [22,23]. Therefore a corneal endothelial cell line developed in this way does not appear to be suitable for the treatment of human corneal diseases. To resolve this problem, we expressed mutant cyclin-dependent kinase (Cdk) 4 and CyclinD1 to inactivate the pRB pathway and generate corneal endothelial cell lines without transducing viral oncogenes.

Results

HCEC with Descemet's membranes were proliferated slowly in a culture dish coated in type IV collagen. After two passages, the cells were transferred into 24-well dishes and transfected with a retroviral vector carrying E6/E7 or mutant Cdk4 and CyclinD1. Three cell lines were successfully generated, as shown in Fig. 1A, with obvious differences in growth (Fig. 1B). Protein expression from the transduced gene was confirmed by western blotting (Fig. 1C). As previously reported [21], THCEC (E6/E7) was immortalized, and THCEC (Cyclin) demonstrated the same proliferative capacity as THCEC (E6/E7), while primary cells grew more slowly even when cultured in 10% fetal bovine serum. These results indicate that induction of mutant Cdk4 and CyclinD1 is sufficient to generate a HCEC line that proliferates at a faster rate than the primary cell line.

Proliferation capacity was also confirmed by immunohistochemistry of Ki-67 (Fig. 2A). Expression of downstream genes of CyclinD1 which are associated with cell proliferation was analyzed by real-time polymerase chain reaction (PCR) (Fig. 2B). Positive staining of Ki-67, which is detected in the nucleus, was confirmed in both THCEC (Cyclin) and THCEC (E6/E7). Real-time PCR also revealed that CDC2 and PCNA, target genes of E2F (an upstream transcriptional factor), that are activated by CyclinD1, were up-regulated in THCEC (E6/E7) and especially in THCEC (Cyclin).

Expression of genes involved in active transmembrane transporter activity, including Na^+/K^+-ATPase, or cell adhesion, including ZO-1 and N-cadherin, were assessed by semi-quantitative reverse transcriptase (RT)-PCR (Fig. 3A). Expression of intercellular adhesion molecules was confirmed by immunohistochemistry (Fig. 3B–J). Semi-quantitative RT-PCR showed that there was no significant difference between the three cell lines regarding the expression of genes associated with several molecules of cell adhesion or of ion transporter channels, which are characteristically expressed by HCEC [21,24]. This was also confirmed by real-time PCR (data not shown).

ZO-1 and N-cadherin, key HCEC adhesion molecules [24], demonstrated positive staining at the intercellular junction in HCEH (Fig. 3F, I) and THCEC (Cyclin) (Fig. 3E, H), while neither ZO-1 nor N-cadherin was detected in THCEC (E6/E7) despite sufficient cellular density (Fig. 3G, J). Although positive staining of ZO-1 and N-cadherin was observed at the intercellular junction in THCEC (Cyclin), ZO-1 staining also occurred around the nucleus (Fig. 3E), indicating the immature distribution of the ZO-1 protein. In THCEC (Cyclin) and HCEC, hexagonal morphology was identified both by phase-contrast micrography (Fig. 3B, C) and immunocytochemistry, while the structure of hexagonal cell shape was not maintained in THCEC (E6/E7) (Fig. 3D). These data indicate that THCEC (Cyclin) and HCEC, but not THCEC (E6/E7), maintain contact inhibition which is crucial for preserving the monolayer.

Scanning electron microscopy was performed to reveal detailed information on the cellular junction (Fig. 4). THCEC (Cyclin) and HCEC showed a clear cellular junction including a tight junction, whereas THCEC (E6/E7) grew as a multilayer without forming a cellular junction, which confirms the immunohistochemistry result.

Representative traces of circuit current driven by the Na^+/K^+-ATPase were of similar shapes in both HCEC and THCEC (Cyclin) (Fig. 5A). These circuit currents maintain corneal translucency and their levels in both cell lines were clearly reduced by the presence of the Na^+/K^+-ATPase inhibitor ouabain, which confirms that the origin of the current is Na^+/K^+-ATPase. Meanwhile, the pump function in THCEC (Cyclin), detected in both earlier and later passages of cells, was more variable than that in HCEC (Fig. 5B), possibly indicating incomplete Na^+/K^+-ATPase activity or the presence of an intercellular barrier that regulates ion permeability. No regular circuit current was detected in THCEC (E6/E7) (Fig. 5A, B), which probably reflects the absence of intercellular adhesion preventing free ion transport across the membrane. This experiment clearly showed that the THCEC (Cyclin) monolayer has similar Na^+/K^+-ATPase activity to that of HCEC.

A tumorigenesis assay of nude mice detected no solid tumor in either THCEC (Cyclin) or THCEC (E6/E7), while HeLa cells formed a solid tumor in all mice (Table 1). Since THCEC (Cyclin) has a similar morphology and pump function to HCEC, THCEC (Cyclin) could be suitable for HCEC studies.

Discussion

THCEC (E6/E7) was shown to achieve immortalization with a highly activated proliferative capacity, as previously described [21]. However, the cell lines did not show normal intercellular contact or normal pump function, probably because contact inhibition in the cell line was not achieved. Meanwhile, THCEC (Cyclin) was demonstrated to have normal physiologic function with a greater proliferative capacity than primary cells, but slightly lower than that of THCEC (E6/E7).

In expanding the cellular life span, E7 has been shown to play a role in the inactivation of pRB, while E6 activates telomerase [25] and accelerates p53 degradation, which induces the Cdk inhibitor p21 [26]. However, little is known about the effector sites of the viral oncogene that may be related to genetic instability of immortalized cells. In the present study, expression of genes specific to HCEC was not drastically different between the three cell lines. However, key proteins including ZO-1 and N-cadherin that are important in forming intercellular contacts were detected, probably because of the unknown influence of viral oncogenes on post-translational modification, posttranslational import or protein stability/degradation.

We recently established genetically stable, non-transformed immortalized ovarian surface epithelium (OSE) cell lines without viral oncogenes by expressing mutant Cdk 4, CyclinD1 and hTERT, based on the hypothesis that inactivation of the pRb pathway and activation of telomerase are sufficient for OSE immortalization [27]. Meanwhile, Rane et al. demonstrated that mutant Cdk 4 (Cdk4R24C) is sufficient to induce carcinogenesis in several other tissues including those of the pancreas, pituitary and brain [28], and Joyce and colleagues showed that HCEC are arrested in the G1 phase and regulated by CKIs, p16INK4a and p21WAF1/Cip1 [29]. Considering the importance of maintaining

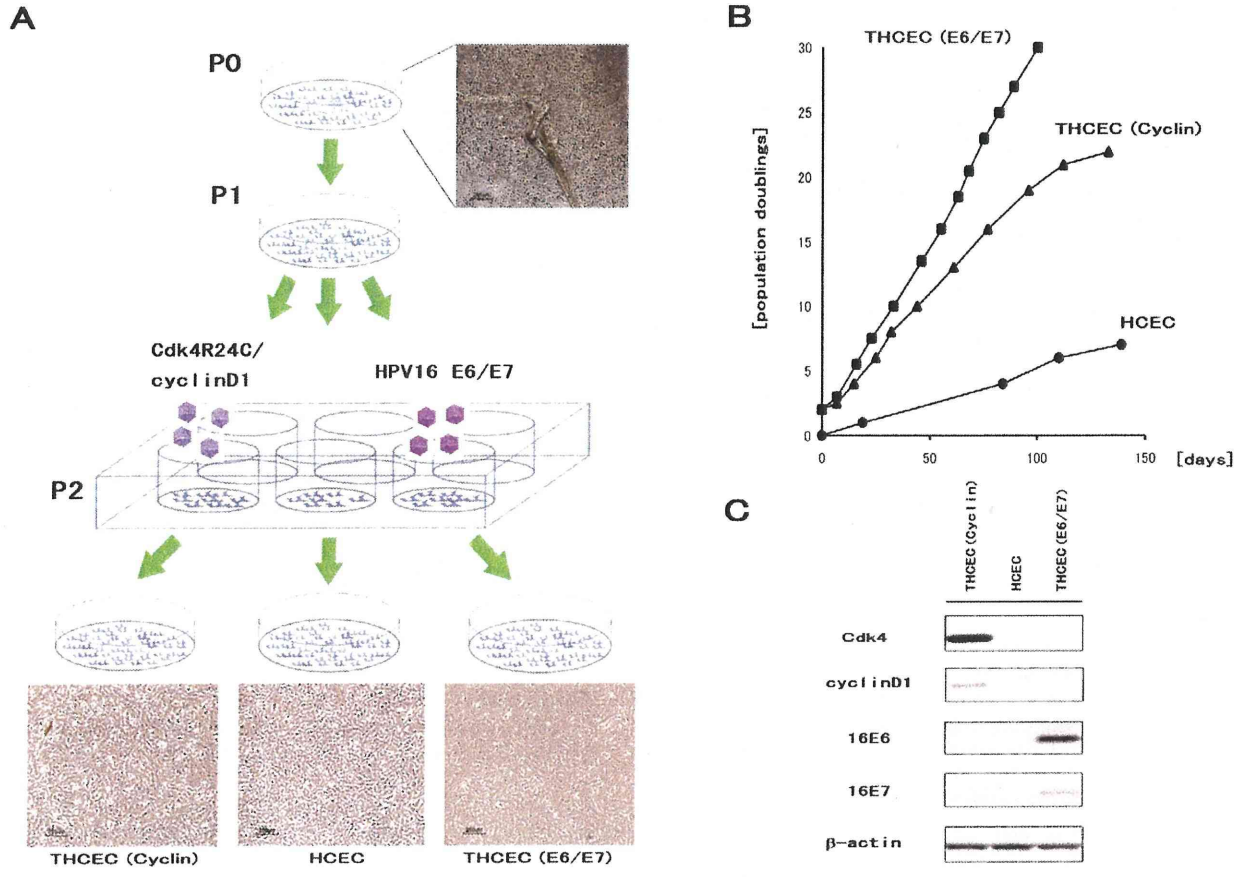

Figure 1. Establishment of THCEC (E6/E7), THCEC (Cyclin) and HCEC. (A) HCEC with Descemet's membrane were placed on Type IV collagen-coated 35 mm cell culture dishes with growth medium (P0). After one passage (P1), retroviral infection was conducted in 6-well cell culture dishes at P2. THCEC (E6/E7) and THCEC (Cyclin) were infected by retroviral vectors carrying HPV16 E6/E7 and both CyclinD1 and Cdk4R24C, respectively. (B) Growth curves of THCEC (E6/E7), THCEC (Cyclin) and HCEC cell lines. THCEC (E6/E7) was immortalized as reported previously, and THCEC (Cyclin) obtained the same proliferative activity as that of THCEC (E6/E7). Transfection was performed on day 0 for THCEC (E6/E7) and THCEC (Cyclin), with population doublings of 2. For HCEC, primary culture commenced on day 0. (C) Western blotting confirmed the expression of the following transgenes: E6 and E7 in THCEC (E6/E7), and CyclinD1 and Cdk4R24C in THCEC (Cyclin).
doi:10.1371/journal.pone.0029677.g001

morphology and physiologic function in HCEC, we only transduced mutant Cdk 4 and CyclinD1, not hTERT, in the present study. We believe that our careful method enabled THCEC (Cyclin) to form a fragile and regularly arranged monolayer complete with physiologic function.

Although THCEC (Cyclin) has similar characteristics to primary HCEC, immunohistochemistry and the Ussing chamber assay also highlighted the differences between the cells. ZO-1 protein was expressed around the nucleus of THCEC (Cyclin) but not in primary cells. Since semi-quantitative PCR detected almost the same level of mRNA expression between the cell lines, staining around the nucleus in THCEC (Cyclin) probably reflects an error in posttranslational import of ZO-1 protein. The Ussing chamber assay detected a similar pump function between THCEC (Cyclin) and primary cells, but the current in THCEC (Cyclin) was more variable than that of the primary cells, which might have been caused by reduced Na^+/K^+-ATPase activity, immature intercellular adhesion allowing irregular intercellular ion transport or differences in cellular density.

Cells established by a retrovirus carry a potential risk of promoting carcinogenesis [30], and direct transplantation to humans of cell sheets composed of such cells may lead to complex problems. Recently, to resolve this problem, several studies have reported the establishment of untransfected corneal endothelial cell lines [31,32,33], which are the most ideal cell lines for the treatment of human corneal disease. Meanwhile, alternative bioengineering approaches, including lipofection of p27kip1 siRNA [34], proteomics technology analyzing the difference between younger and older HCEC [35] and drug usage of promyelocytic leukemia zinc finger protein, a cell cycle transcriptional repressor and negative regulator [36], have also been introduced. The present findings support the idea that targeting the interaction between p16INK4a and Cdk4 using such methods is a promising strategy to generate HCEC with sufficient proliferative capacity and physiologic function.

Materials and Methods

Isolation and cell culture of human corneal cells

Ethics Statement. A cornea was excised from the surgically enucleated eye of a 2-year-old infant undergoing therapy for retinoblastoma, with the approval (approval number, #156) of the

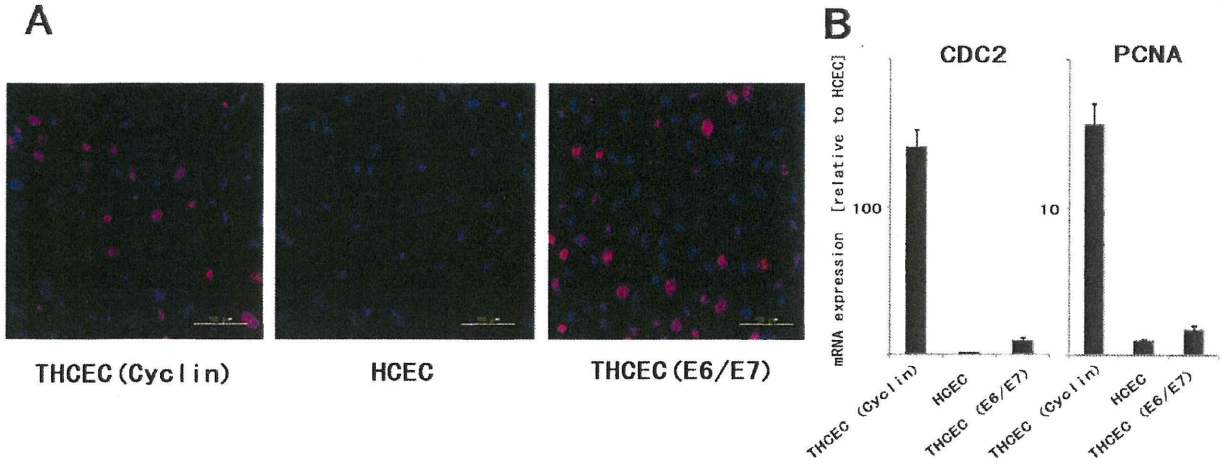

Figure 2. Evaluation of proliferative capacity. (A) Immunohistochemistry of Ki-67 in three cell lines. Positive staining of Ki-67, located in the nucleus, was obviously identified in THCEC (Cyclin) and THCEC (E6/E7), but rarely detected in HCEC. (B) Real-time PCR of downstream genes of cyclinD1 associated with proliferation. Gene expression levels of both CDC2 and PCAN were clearly higher than that of HCEC. The gene expression was much more activated in THCEC (Cyclin) in which the expression of E2F, an upstream transcriptional factor of two genes, was constitutively activated by transduced mutant Cdk4 and CyclinD1.
doi:10.1371/journal.pone.0029677.g002

Ethics Committee of the National Institute for Child and Health Development, Tokyo, Japan. Signed informed consent was obtained from the donor's parents, and the surgical specimens were irreversibly de-identified. All experiments handling human cells and tissues were performed in line with the tenets of the Declaration of Helsinki.

The corneal piece, which was grossly normal with no pathological lesions, was cut 1.5 mm from the corneal limbus,

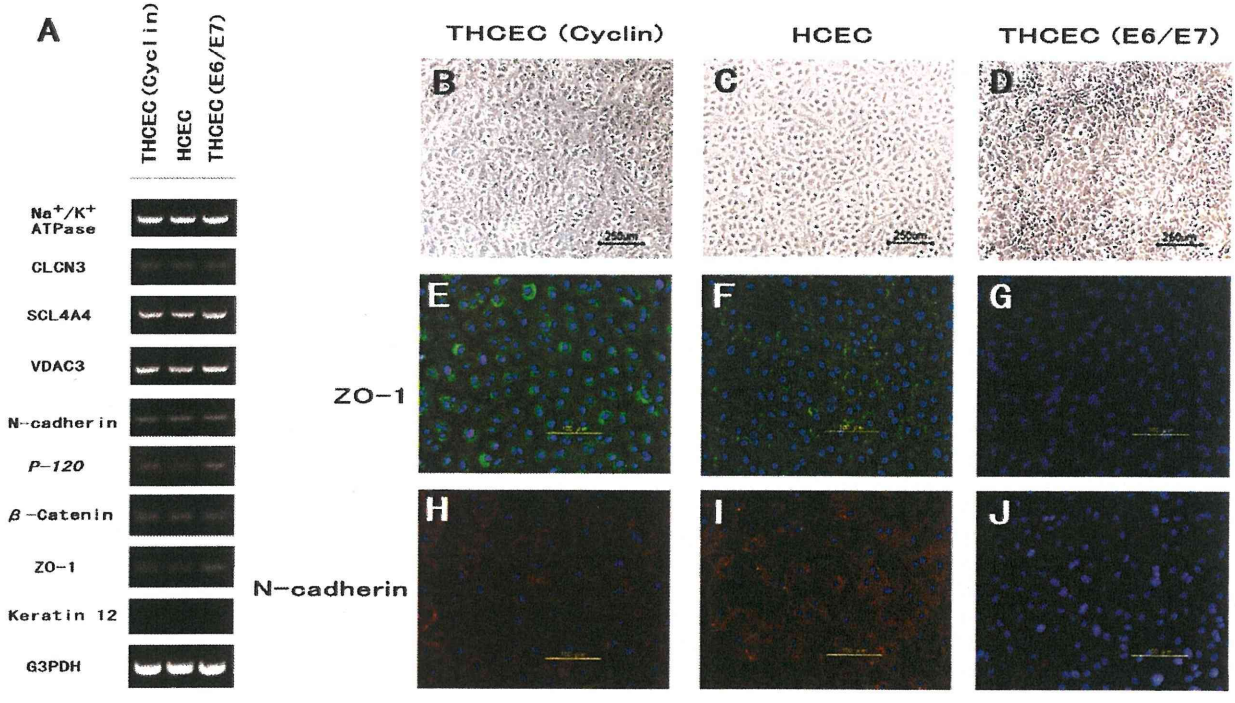

Figure 3. HCEC-associated genes and cytolocalization of junctional components expressed by cell lines. (A) Semi-quantitative reverse transcriptase polymerase chain reaction for HCEC-associated genes. Total RNA was prepared from cultured cells seven days after reaching confluency. No significant difference in mRNA expression was observed between the three cell lines. Compared with phase-contrast micrographs of (B) THCEC (Cyclin), (C) HCEC and (D) THCEC (E6/E7), cytolocalization was examined by immunofluorescence staining of ZO-1 (E, F,G) and N-cadherin (H, I, J). THCEC (E6/E7) did not stain positive for intercellular junctional molecules, while ZO-1 and N-cadherin stained positive at the junction in THCEC (Cyclin) and HCEC.
doi:10.1371/journal.pone.0029677.g003

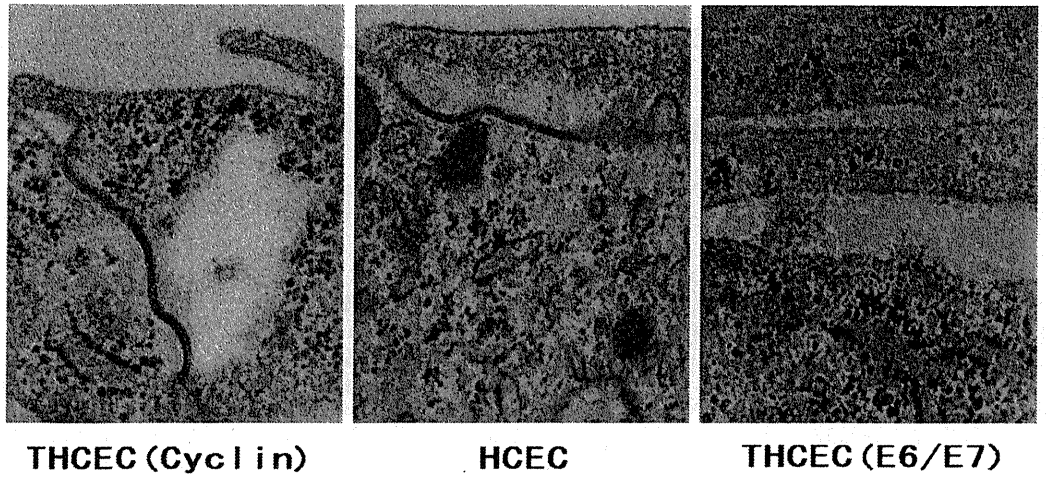

Figure 4. Transmission electron microscopy of cell line intercellular junctions. The junctional complex was detected at the intercellular junction in THCEC (Cyclin) and HCEC. No component of the intercellular junction was found in THCEC (E6/E7), in which cells grew in multilayers without being inhibited by cellular contact (scale bar = 200 nm).
doi:10.1371/journal.pone.0029677.g004

avoiding contamination of the trabecular meshwork tissue. HCEC with Descemet's membrane were stripped from the posterior surface of the corneal tissue with sterile surgical forceps under a dissecting microscope. They were cut into two pieces and cultured in a cell culture dish covered with Type IV collagen in a growth medium (GM); Dulbecco's modified Eagle's medium (DMEM)/ Nutrient mixture F12 (1:1) with high glucose supplemented with 10% fetal bovine serum, insulin-transferrin-selenium and MEM-NEAA (Gibco, Auckland, NZ). Cells were subcultured after reaching confluency by treating with trypsin/EDTA and seeded at a density of 5×10^5 cells/well in 6-well dishes.

Viral vector construction and viral transduction

Lentiviral vector plasmids, CSII-CMV-cyclin D1 and -CDK4R24C were constructed by recombination using the Gateway system (Invitrogen, Carlsbad, CA) as described previously [37]. Briefly, cDNAs of human cyclinD1 and a mutant form of Cdk4 (Cdk4R24C: an inhibitor resistant form of Cdk4, generously provided by Dr Hara) were recombined with a lentiviral vector, CSII-CMV-RfA (a gift from Dr Miyoshi), by LR reaction to create a Gateway expression plasmid (Invitrogen) according to the manufacturer's instructions.

Previous work has described the production of recombinant lentiviruses with the vesicular stomatitis virus G glycoprotein [37], the recombinant retrovirus vector plasmid, pCLXSN-16E6E7 encoding HPV16 E6/E7 (16E6E7) [38] and recombinant retroviruses [39]. Following the addition of recombinant viral fluid to cells seeded in 24-well dishes in the presence of 4 μg/ml polybrene, the cells were infected by the viruses. Stably transduced cells with an expanded life span were designated transduced

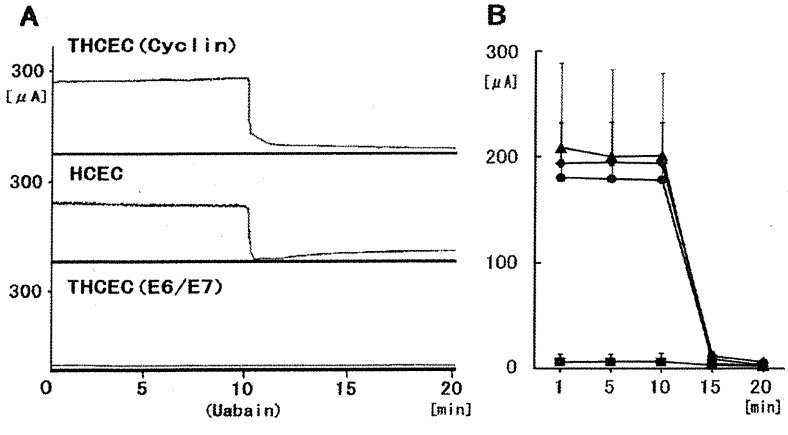

Figure 5. The pump function of cell lines. Short-circuit currents representing Na^+/K^+-ATPase activity from corneal cell monolayers on the insert well area of 4.67 cm^2 were calculated before and after addition of the Na^+/K^+-ATPase inhibitor ouabain. (A) Representative tracings of short-circuit current (μA/well) obtained with cell monolayers of THCEC (Cyclin) (upper panel), HCEC (middle panel) and THCEC (E6/E7) (lower panel). THCEC (Cyclin) possessed equal transport activity to HCEC, whereas no pump function was detected in THCEC (E6/E7). (B) Time-course changes in the average short circuit current of cultured monolayers of cell lines at 1, 5, 10 and 20 min. Data shown are for (▲) THCEC (Cyclin) at PD8, (♦) THCEC (Cyclin) at PD 21, (•) HCEC and (■) THCEC (E6/E7); all data are expressed as mean±SD of four replicate experiments of each cell line.
doi:10.1371/journal.pone.0029677.g005

Table 1. Tumorigenesis assay of cell lines in BALB/C nude mice.

Inoculated cells	Total dose (cell/mouse)	Number of mice (% mortality)	Number of mice with tumor
THCEC (Cyclin)	1.7×10^6	3(0)	0
THCEC (E6/E7)	1.7×10^6	3(0)	0
HeLa cells	2.0×10^6	3(0)	3

doi:10.1371/journal.pone.0029677.t001

human corneal endothelial cell by E6/E7 (THCEC (E6/E7)) and transduced human corneal endothelial cell by Cdk4R24C/cyclinD1 (THCEH (Cyclin)).

Culture of transfected cell lines and growth curve

When the cultures reached subconfluence, the cells were harvested with 0.25% trypsin and 1 mM EDTA, collected into tubes, and centrifuged. The cells were counted using a cell viability analyzer (Vi-CELL Cell Viability Analyzer, Beckman Coulter, Brea, CA), and population doubling (PD) was calculated. The pellets were suspended in growth medium, and the cells were passaged at a density of 5×10^5 cells/well in a 100-mm dish. The original cells were regarded as PD 2 (day 0).

Western blot analysis

Western blotting was conducted as described previously [40]. Antibodies against Cdk4 (ser473; Cell Signaling Technology, Danvers, MA), CyclinD1 (clone G124-326; BD Biosciences, Franklin Lakes, NJ), β-actin (sc-1616; Santa Cruz Biotechnology, Santa Cruz, CA) were used as probes, and horseradish peroxidase-conjugated anti-mouse, anti-rabbit (Jackson Immunoresearch Laboratories, West Grove, PA) or anti-goat (sc-2033; Santa Cruz Biotechnology, Santa Cruz, CA) immunoglobulins were employed as secondary antibodies.

Immunocytochemistry

Cell lines were grown on Type IV collagen-coated glass dishes 14 days after reaching confluency and were fixed with 4% formaldehyde (pH 7.0) for 15 min at room temperature. Cell lines were then rehydrated in phosphate buffered saline (PBS), incubated with 0.2% Triton X-100 for 15 min and rinsed three times with PBS for 5 min each. After incubation with 2% BSA to block nonspecific staining for 30 min, cell lines were incubated with anti-ZO-1 (1:50; sc-8146; Santa Cruz Biotechnology, Santa Cruz, CA), anti-N-cadherin (1:50; sc-7939; Santa Cruz Biotechnology) and anti-Ki67 (1:100; ab15580; Abcam, Cambridge, UK) for 16 h at 4°C. After three washes with PBS, cell lines were incubated with the secondary antibody for 60 min, followed by counterstaining with 4′,6-diamidino-2-phenylindole (1:200; sc-3598; Santa Cruz Biotechnology) for 10 min.

Semi-quantitative RT-PCR

Total RNA was extracted from 1×10^6 cultured HCEC using the RNeasy Plus mini-kitH (Qiagen, Germantown/Gaithersburg, MA) according to the manufacturer's instructions and quantified by absorption at 260 nm. Total RNA was then reverse-transcribed into cDNA using Superscript III Reverse Transcriptase (Invitrogen, Carlsbad, CA) with oligo random hexamers. cDNAs of each component were amplified by PCR using specific primers and DNA polymerase. The reaction was first incubated at 95°C for 10 min, followed by 39 cycles at 98°C for 30 s, 58°C for 30 s and 74°C for 30 s. PCR primers are listed in Table 2.

Quantitative real-time RT-PCR

Total RNA extraction and reverse transcription into cDNA was carried out as above. Each quantitative real-time RT-PCR for target genes, including Cell Division Cycle 2 (*CDC2*) and proliferating cell nuclear antigen (*PCNA*), was performed using the Chromo4 real time detection system (Bio-Rad, Hercules, CA). For a 20 ml PCR, the cDNA template was mixed with the primers to final concentrations of 200 nM and 10 µl of SsoFast EvaGreen Supermix (BIO-RAD), respectively. The reaction was first incubated at 95°C for 10 min, followed by 45 cycles at 95°C for 10 s, 57°C for 15 s, and 72°C for 20 s.

Transmission Electron Microscopy

Cell lines cultured on Type IV collagen-coated dishes were fixed in HEPES buffered 2% glutaraldehyde and subsequently post-fixed in 2% osmium tetroxide for 3 h on ice. Specimens were then dehydrated in graded ethanol and embedded in the epoxy resin. Ultrathin sections were obtained by ultramicrotomy and stained with uranyl acetate for 10 min and modified Sato's lead solution for 5 min then submitted to TEM observation (JEM-2000EX, JEOL).

Measurement of pump function

The pump function of confluent monolayers of HCEC was measured using an Ussing chamber as described previously [41]. Cells cultured on Snapwell inserts coated with Type IV collagen were placed in the Ussing chamber EM-CSYS-2 (Physiologic Instruments, San Diego, CA) with the endothelial cell surface side in contact with one chamber and the Snapwell membrane side in contact with another chamber. The chambers were carefully filled with Krebs-Ringer bicarbonate (120.7 mM NaCl, 24 mM $NaHCO_3$, 4.6 mM KCl, 0.5 mM $MgCl_2$, 0.7 mM Na_2HPO_4, 1.5 mM NaH_2PO_4 and 10 mM glucose bubbled with a mixture of 5% CO_2, 7% O_2 and 88% N_2 to pH 7.4). The chambers were maintained at 37°C using an attached heater.

The short-circuit current was sensed by narrow polyethylene tubes positioned close to either side of the Snapwell, filled with 3 M KCl and 4% agar gel and connected to silver electrodes. These electrodes were connected to the computer through the Ussing system VCC-MC2 (Physiologic Instruments) and an iWorx 118 Research Grade Recorder (iWorx Systems, Dover, NH), and the short-circuit current was recorded by Labscribe2 Software for Research (iWorx). After the short-circuit current had reached a steady state, ouabain (final concentration, 1 mM) was added to the chamber, and the short-circuit current was re-measured. The pump function attributable to Na^+/K^+-ATPase activity was calculated as the difference in short-circuit current measured before and after the addition of ouabain.

Tumorigenesis assay

Cells were harvested by Trypsin/EDTA treatment, collected into tubes, and centrifuged, and the pellets were suspended in

Table 2. Oligonucleotide sequences for RT-PCR.

Name	Sequence	Size (bp)	Accession Number
Collagen type IV	F: 5′-GGC ACC TGC CAC TAC TAC GC-3′	472	NM_001845
	R: 5′-TCA CCA GGA GGT AGC CGA T-3′		
Keratin 12	F: 5′-GAT GCT AAT GCT GAG CTC GA-3′	393	NM_000223
	R: 5′-ACC TGC CCT ACA GCT TTG TA-3		
VDAC3	F: 5′-TGA CTC TTG ATA CCA TAT TTG TAC CG-3′	482	NM_001135694
	R: 5′-TCA ATT TGA CTC CTG GTC GAA-3′		
CLCN3	F: 5′-AGA AAG GCA TAG ACG GAT CAA-3′	204	NM_001829
	R: 5′-GGT TGT ACC ACA ACG CAC TAA-3′		
SLC4A4	F: 5′-GTT CAG ATG AAT GGG GAT ACGC	697	NM_001136260
	R: 5′-CGA GCA TAA ACA CAA AGC GTA A-3′		
Na^+/K^+-ATPase	F: 5′-CCC AGG ACT CAT GGT TTT TC-3′	482	NM_000702
	R: 5′-GGA GCA AAG CTG ACC TGA AC-3′		
N-cadherin	F: 5′-CAA CTT GCC AGA AAA CTC CAG G-3′	205	NM_ 001792
	R: 5′-ATG AAA CCG GGC TAT CTG CTC-3′		
β-catenin	F: 5′-TAC CTC CCA AGT CCT GTA TGA G-3′	180	NM _001904
	R: 5′-TGA GCA GCA TCA AAC TGT GTA G-3′		
P-120	F: 5′-CCC CAG GAT CAC AGT CAC CT-3′	144	NM_001085467
	R: 5′-CCG AGT GGT CCC ATC ATC TG-3′		
ZO-1	F: 5′-AGT CCC TTA CCT TTC GCC TGA-3′	180	NM_003257
	R: 5′-TCT CTT AGC ATT ATG TGA GCT GC-3′		
GAPDH	F: 5′-GCT CAG ACA CCA TGG GGA AGG T-3′	474	NM_002046
	R: 5′-GTG GTG CAG GAG GCA TTG CTG A-3′		
PCNA	F: 5′- GCGTGAACCTCACCAGTATGT-3′	76	NM_002592
	R: 5′- TCTTCGGCCCTTAGTGTAATGAT-3′		
CDC2	F: 5′- GGATGTGCTTATGCAGGATTCC-3′	100	NM_001786
	R: 5′- CATGTACTGACCAGGAGGGATAG-3′		

VDAC3: voltage-dependent anion channel 3, CLCN3: chloride channel protein 3, SLC4A4: sodium bicarbonate cotransporter membrane.
doi:10.1371/journal.pone.0029677.t002

DMEM. The same volume of Basement Membrane Matrix (BD Biosciences) was added to the cell suspension. Cells (1.7×10^6) of THCEC (Cyclin) and THCEC (E6/E7) were inoculated subcutaneously into dorsal flanks of each of three Balb/c nu/nu mice (CREA, Japan) for 60 days. A total of 2.0×10^6 HeLa cells per mouse were used as positive controls. The skin of dorsal flanks of inoculated mice was surgically opened and the tumorigenic status was examined.

Author Contributions

Conceived and designed the experiments: Tadashi Yokoi YS Tae Yokoi TK AU HN NA. Performed the experiments: Tadashi Yokoi YS Tae Yokoi HM SH MY TK HN NA. Analyzed the data: Tadashi Yokoi YS Tae Yokoi HM SH MY AU HN NA. Contributed reagents/materials/analysis tools: Tadashi Yokoi SH MY TK HN NA. Wrote the paper: Tadashi Yokoi YS TK AU HN NA.

References

1. Hatou S, Yamada M, Mochizuki H, Shiraishi A, Joko T, et al. (2009) The effects of dexamethasone on the Na,K-ATPase activity and pump function of corneal endothelial cells. Curr Eye Res 34: 347–354.
2. Barfort P, Maurice D (1974) Electrical potential and fluid transport across the corneal endothelium. Exp Eye Res 19: 11–19.
3. Bourne WM, Nelson LR, Hodge DO (1997) Central corneal endothelial cell changes over a ten-year period. Invest Ophthalmol Vis Sci 38: 779–782.
4. Hashemian MN, Moghimi S, Fard MA, Fallah MR, Mansouri MR (2006) Corneal endothelial cell density and morphology in normal Iranian eyes. BMC Ophthalmol 6: 9.
5. Padilla MD, Sibayan SA, Gonzales CS (2004) Corneal endothelial cell density and morphology in normal Filipino eyes. Cornea 23: 129–135.
6. Adamis AP, Filatov V, Tripathi BJ, Tripathi RC (1993) Fuchs' endothelial dystrophy of the cornea. Surv Ophthalmol 38: 149–168.
7. Schultz RO, Matsuda M, Yee RW, Edelhauser HF, Schultz KJ (1984) Corneal endothelial changes in type I and type II diabetes mellitus. Am J Ophthalmol 98: 401–410.
8. Slingsby JG, Forstot SL (1981) Effect of blunt trauma on the corneal endothelium. Arch Ophthalmol 99: 1041–1043.
9. Bourne WM, Nelson LR, Hodge DO (1994) Continued endothelial cell loss ten years after lens implantation. Ophthalmology 101: 1014–1022;discussion 1022–1013.
10. Gagnon MM, Boisjoly HM, Brunette I, Charest M, Amyot M (1997) Corneal endothelial cell density in glaucoma. Cornea 16: 314–318.
11. Laing RA, Sanstrom MM, Berrospi AR, Leibowitz HM (1976) Changes in the corneal endothelium as a function of age. Exp Eye Res 22: 587–594.
12. Landshman N, Ben-Hanan I, Assia E, Ben-Chaim O, Belkin M (1988) Relationship between morphology and functional ability of regenerated corneal endothelium. Invest Ophthalmol Vis Sci 29: 1100–1109.
13. Coster DJ, Williams KA (2005) The impact of corneal allograft rejection on the long-term outcome of corneal transplantation. Am J Ophthalmol 140: 1112–1122.
14. Terry MA, Ousley PJ (2001) Deep lamellar endothelial keratoplasty in the first United States patients: early clinical results. Cornea 20: 239–243.
15. Price FW Jr., Price MO (2005) Descemet's stripping with endothelial keratoplasty in 50 eyes: a refractive neutral corneal transplant. J Refract Surg 21: 339–345.
16. Melles GR, Ong TS, Ververs B, van der Wees J (2006) Descemet membrane endothelial keratoplasty (DMEK). Cornea 25: 987–990.

17. Zhu C, Joyce NC (2004) Proliferative response of corneal endothelial cells from young and older donors. Invest Ophthalmol Vis Sci 45: 1743–1751.
18. Li W, Sabater AL, Chen YT, Hayashida Y, Chen SY, et al. (2007) A novel method of isolation, preservation, and expansion of human corneal endothelial cells. Invest Ophthalmol Vis Sci 48: 614–620.
19. Ishino Y, Zhu C, Harris DL, Joyce NC (2008) Protein tyrosine phosphatase-1B (PTP1B) helps regulate EGF-induced stimulation of S-phase entry in human corneal endothelial cells. Mol Vis 14: 61–70.
20. Senoo T, Joyce NC (2000) Cell cycle kinetics in corneal endothelium from old and young donors. Invest Ophthalmol Vis Sci 41: 660–667.
21. Kim HJ, Ryu YH, Ahn JI, Park JK, Kim JC (2006) Characterization of immortalized human corneal endothelial cell line using HPV 16 E6/E7 on lyophilized human amniotic membrane. Korean J Ophthalmol 20: 47–54.
22. Nitta M, Katabuchi H, Ohtake H, Tashiro H, Yamaizumi M, et al. (2001) Characterization and tumorigenicity of human ovarian surface epithelial cells immortalized by SV40 large T antigen. Gynecol Oncol 81: 10–17.
23. Tsao SW, Mok SC, Fey EG, Fletcher JA, Wan TS, et al. (1995) Characterization of human ovarian surface epithelial cells immortalized by human papilloma viral oncogenes (HPV-E6E7 ORFs). Exp Cell Res 218: 499–507.
24. Zhu YT, Hayashida Y, Kheirkhah A, He H, Chen SY, et al. (2008) Characterization and comparison of intercellular adherent junctions expressed by human corneal endothelial cells in vivo and in vitro. Invest Ophthalmol Vis Sci 49: 3879–3886.
25. Kiyono T, Foster SA, Koop JI, McDougall JK, Galloway DA, et al. (1998) Both Rb/p16INK4a inactivation and telomerase activity are required to immortalize human epithelial cells. Nature 396: 84–88.
26. Sekiguchi T, Hunter T (1998) Induction of growth arrest and cell death by overexpression of the cyclin-Cdk inhibitor p21 in hamster BHK21 cells. Oncogene 16: 369–380.
27. Sasaki R, Narisawa-Saito M, Yugawa T, Fujita M, Tashiro H, et al. (2009) Oncogenic transformation of human ovarian surface epithelial cells with defined cellular oncogenes. Carcinogenesis 30: 423–431.
28. Rane SG, Cosenza SC, Mettus RV, Reddy EP (2002) Germ line transmission of the Cdk4(R24C) mutation facilitates tumorigenesis and escape from cellular senescence. Mol Cell Biol 22: 644–656.
29. Enomoto K, Mimura T, Harris DL, Joyce NC (2006) Age differences in cyclin-dependent kinase inhibitor expression and rb hyperphosphorylation in human corneal endothelial cells. Invest Ophthalmol Vis Sci 47: 4330–4340.
30. Robinson HL (1982) Retroviruses and cancer. Rev Infect Dis 4: 1015–1025.
31. Fan T, Zhao J, Ma X, Xu X, Zhao W, et al. (2011) Establishment of a continuous untransfected human corneal endothelial cell line and its biocompatibility to denuded amniotic membrane. Mol Vis 17: 469–480.
32. Fan T, Wang D, Zhao J, Wang J, Fu Y, et al. (2009) Establishment and characterization of a novel untransfected corneal endothelial cell line from New Zealand white rabbits. Mol Vis 15: 1070–1078.
33. Valtink M, Gruschwitz R, Funk RH, Engelmann K (2008) Two clonal cell lines of immortalized human corneal endothelial cells show either differentiated or precursor cell characteristics. Cells Tissues Organs 187: 286–294.
34. Kikuchi M, Zhu C, Senoo T, Obara Y, Joyce NC (2006) p27kip1 siRNA induces proliferation in corneal endothelial cells from young but not older donors. Invest Ophthalmol Vis Sci 47: 4803–4809.
35. Zhu C, Rawe I, Joyce NC (2008) Differential protein expression in human corneal endothelial cells cultured from young and older donors. Mol Vis 14: 1805–1814.
36. Shiraishi A, Joko T, Higashiyama S, Ohashi Y (2007) Role of promyelocytic leukemia zinc finger protein in proliferation of cultured human corneal endothelial cells. Cornea 26: S55–58.
37. Miyoshi H, Blomer U, Takahashi M, Gage FH, Verma IM (1998) Development of a self-inactivating lentivirus vector. J Virol 72: 8150–8157.
38. Narisawa-Saito M, Yoshimatsu Y, Ohno S, Yugawa T, Egawa N, et al. (2008) An in vitro multistep carcinogenesis model for human cervical cancer. Cancer Res 68: 5699–5705.
39. Naviaux RK, Costanzi E, Haas M, Verma IM (1996) The pCL vector system: rapid production of helper-free, high-titer, recombinant retroviruses. J Virol 70: 5701–5705.
40. Haga K, Ohno S, Yugawa T, Narisawa-Saito M, Fujita M, et al. (2007) Efficient immortalization of primary human cells by p16INK4a-specific short hairpin RNA or Bmi-1, combined with introduction of hTERT. Cancer Sci 98: 147–154.
41. Mimura T, Yamagami S, Yokoo S, Usui T, Tanaka K, et al. (2004) Cultured human corneal endothelial cell transplantation with a collagen sheet in a rabbit model. Invest Ophthalmol Vis Sci 45: 2992–2997.

Carcinogenesis Advance Access published March 1, 2012
Carcinogenesis vol.0 no.0 pp.1–8, 2012
doi:10.1093/carcin/bgs104
Advance Access publication February 15, 2012

A critical role of MYC for transformation of human cells by HPV16 E6E7 and oncogenic HRAS

Mako Narisawa-Saito[1,†], Yuki Inagawa[1,†], Yuki Yoshimatsu[1], Kei haga[1], Katsuyuki Tanaka[1], Nagayasu Egawa[1], Shin-ichi Ohno[1], Hitoshi Ichikawa[2], Takashi Yugawa[1], Masatoshi Fujita[1,3] and Tohru Kiyono[1,*]

[1]Division of Virology and [2]Division of Genetics, National Cancer Center Research Institute, 5-1-1 Tsukiji, Chuo-ku, Tokyo 104-0045, Japan and [3]Department of Cellular Biochemistry, Graduate School of Pharmaceutical Sciences, Kyushu University, 3-1-1 Maidashi, Higashi-ku, Fukuoka 812-8582, Japan

*To whom correspondence should be addressed. Tel: +81 3 3547 5275; Fax: +81 3 3543 2181; Email: tkiyono@ncc.go.jp

Human papillomaviruses (HPVs) are the primary causal agents for development of cervical cancer, and deregulated expression of two viral oncogenes E6 and E7 is considered to contribute to disease initiation. Recently, we have demonstrated that transduction of oncogenic HRAS ($HRAS^{G12V}$) and MYC together with HPV16 E6E7 is sufficient for tumorigenic transformation of normal human cervical keratinocytes (HCKs). Here, we show that transduction of $HRAS^{G12V}$ on the background of E6E7 expression causes accumulation of MYC protein and tumorigenic transformation of not only normal HCKs but also other normal primary human cells, including tongue keratinocytes and bronchial epithelial cells as well as hTERT-immortalized foreskin fibroblasts. Subcutaneous transplantation of as few as 200 HCKs expressing E6E7 and $HRAS^{G12V}$ resulted in tumor formation within 2 months. Dissecting RAS signaling pathways, constitutively active forms of AKT1 or MEK1 did not result in tumor formation with E6E7, but tumorigenic transformation was induced with addition of MYC. Increased MYC expression endowed resistance to calcium- and serum-induced terminal differentiation and activated the mammalian target of rapamycin (mTOR) pathway. An mTOR inhibitor (Rapamycin) and MYC inhibition a level not affecting proliferation in culture both markedly suppressed tumor formation by HCKs expressing E6E7 and $HRAS^{G12V}$. These results suggest that a single mutation of HRAS could be oncogenic in the background of deregulated expression of E6E7 and MYC plays a critical role in cooperation with the RAS signaling pathways in tumorigenesis. Thus inhibition of MYC and/or the downstream mTOR pathway could be a therapeutic strategy not only for the MYC-altered but also RAS-activated cancers.

Introduction

A subset of human papillomaviruses (HPVs), the so called high-risk types such as type 16 and 18, are associated with >90% of all cervical carcinomas as primary causal agents (1), with deregulated expression of the HPV viral oncogenes E6 and E7 as the main contributors to an etiology (2). However, epidemiological studies and experimental data indicate that the viral presence is not enough to induce cervical cancer and additional genetic and epigenetic events (to alter the cellular factors) are presumably required (3). To address this, we have established an *in vitro* model for cervical cancer with normal human cervical keratinocytes (HCKs) focusing on sequential transduction of defined genetic elements (4) and succeeded in the creation of highly potent cancer initiating cells by introduction of c-MYC (MYC) and oncogenic $HRAS^{G12V}$ (HRAS) on a background of HPV16 E6 and E7 expression (4). However, since the cells having been cultivated in the differentiating medium were used for the assays, we could not exclude the possibility that genetic and/or epigenetic alterations during the selection might be critical for the transformation. In the present study, by directly examining transformed phenotype of the cells without such selection, we could demonstrate that oncogenic HRAS, without overexpression of exogenous MYC, is sufficient for tumorigenic transformation of normal human cells expressing E6 and E7. Nonetheless, endogenous MYC stabilized by HRAS was revealed to be a critical player in tumor-initiating potential.

Abbreviations: DMEM, Dulbecco's modified Eagle's medium; ERK, extracellular signal-regulated kinase; ES, embryonic stem cell; HBEC, human bronchial epithelial cell; HCK, human cervical keratinocyte; HFF, human foreskin fibroblast; HPV, human papillomavirus; KGM, keratinocyte growth medium; mTOR, mammalian target of rapamycin.

†These authors contributed equally to this work.

Materials and methods

Cell culture and cell lines

Normal HCKs were obtained with written consent from patients who underwent abdominal surgery for a gynecological disease other than cervical cancer. HCK1, HCK4 and HCK8 cells derived from different donors were maintained in low-calcium serum-free keratinocyte growth medium (KGM) (Epilife-KG2 KURABO Industries, Ltd, Osaka, Japan) unless otherwise described. HCK1T cells were established by transduction of *hTERT* into HCK1 cells (4). These HCK cells were then further transduced with HPV16 *E6E7* followed by the oncogene(s) of interest. Normal human bronchial epithelial cells (HBECs) were purchased from Cell Applications (San Diego) and cultivated in KGM. Normal human foreskin fibroblasts (HFFs) purchased from BioWhittaker (Walkersville) were immortalized by transduction of *hTERT*. HFFs and cervical cancer cell lines, SiHa, CaSki and HeLa and C33A, were grown in Dulbecco's modified Eagle's medium (DMEM) (Sigma) containing 10% fetal bovine serum. The source, authentication and methods of maintenance of the cell lines are described in the Supplementary Materials and Methods, available at *Carcinogenesis* Online.

Vector construction and retroviral infection

Construction of the retroviral expression vectors, pCLXSN-16E6E7, pCLXSH-hTERT, pCMSCVpuro-MYC, pCLMSCV-puro-BCL2, pCMSCVpuro-myr-AKT1, pCMSCVbsd-$HRAS^{G12V}$, pCMSCVbsd and pCMSCVpuro-MEK1DD was as described previously (4,5). OmoMYC, a human version of the dominant-interfering MYC mutant (6), which encodes the C-terminal 92 amino acids of MYC with four amino acid substitutions (E410T, E417I, R423Q and R424N) and MYC^{T58A} were made by *in vitro* mutagenesis and cloned into a lentiviral vector, CSII-TRE-Tight-RfA, in which the elongation factor promoter in CSII-EF-RfA (a gift from Hiroyuki Miyoshi, RIKEN, BioResource Center) was replaced with the tetracycline-responsive promoter from pTRE-Tight (Clonetech). CSII-TRE-Tight-16E6E7-2A-MYC^{T58A}-2A-$HRAS^{G12V}$ was constructed by inserting the 16E6E7, MYC^{T58A} and $HRAS^{G12V}$ segments separated by the sequences encoding the autonomous 'self-cleaving' 2A peptides derived from foot-and-mouse disease virus (7) into CSII-TRE-Tight-RfA. CSII-TRE-Tight-MYCmiR-1, -2 and -3 were constructed by inserting the micro RNA sequence based on the BLOCK-iT Pol II miR RNAi system (Invitrogen) into CSII-TRE-Tight-RfA. The target sequence for MYCmiR-1, -2 and -3 are 5′-TAGTCGAGGTCATAGTTCCTG-3′, 5′-ATGAAACTCTGGTTCACCATG-3′ and 5′-TTGACATTCTCCTCGGTGTCC-3′, respectively. The production of recombinant viruses and selection of infected HCKs were detailed earlier (4,5).

Western analysis

Western blotting was conducted as described previously (4). Antibodies used were listed in the Supplementary Material and Methods, available at *Carcinogenesis* Online.

Colony formation in soft agar medium

Cells were seeded at 5×10^4 cells per 35 mm dish (BD-Falcon 3046) in an appropriate medium. Colonies over 50 μm in diameter were counted after 3 weeks as described previously (4).

Clonogenic assay

Aliquots of 500 cells were seeded on 35 mm dishes under sparse conditions. After cultivation for 2 weeks, the cells were stained with Giemsa's dye, and the number of colonies was counted.

Tumorigenesis in nude mice

All surgical procedures and care administered to the animals were in accordance with institutional guidelines. A 100 µl volume of cells in a 1:1 mixture of Matrigel (BD Biosciences) was subcutaneously injected into female BALB/c nude mice (Clea Japan). The expression of human involucrin in all tumors was determined by western blots with antibodies against human involucrin that do not react with mouse epidermis to confirm that the tumors were derived from implanted HCKs (data not shown).

Quantitative reverse transcription–PCR analysis

Quantitative reverse transcription–PCR was performed as described previously (8). Amplified products were detected with a TaqMan Gene Expression Assay (Applied Biosystems). The expression level of the MYC gene was then normalized to RNA content for each sample using beta-2-microglobulin messenger RNA as a control.

Results

Oncogenic HRAS is sufficient for tumor initiation with normal human cells expressing HPV16 E6E7

Previously, we demonstrated that introduction of HPV16 *E6* and *E7* (E6E7), *H-RAS^{G12V}* (HRAS) and *c-MYC* (MYC) to normal HCKs transduced with hTERT (HCK1T) resulted in the creation of highly potent tumor-initiating cells capable of forming tumors in nude mice when only 10 cells were transplanted subcutaneously (4). Since the cells having been cultivated in the differentiating medium containing high calcium and serum (DMEM + 10% fetal bovine serum; DMEM hereafter) were used for the assays, it is possible that such adaptation or selection was required for the tumor-initiating potential by adding further epigenetic or even genetic alteration(s). To exclude the possibility, we directly examined transformed phenotype of the cells soon after transduction of oncogenes cultivated in KGM and revealed that HRAS addition was sufficient for tumorigenic transformation of primary HCKs and HCKTs (HCKT where T is for hTERT) expressing HPV16 E6E7 (Table I, A). In the presence of HRAS, endogenous MYC protein levels were markedly elevated (Figure 1A). When 1 million cells were subcutaneously transplanted into nude mice, HCK4T-E (E is for E6E7) expressing HRAS formed large tumors within 2 weeks, irrespective of the presence of an exogenous MYC transgene although growth was marginally faster with the latter (Figure 1B; $P > 0.05$). A high proportion of tumor-initiating cells in populations expressing E6E7 and HRAS was confirmed by injecting only 200 cells of different batches of HCKTs expressing the same set of genes into nude mice, resulting in tumor formation within 2 months (Table I, B). Thus, we examined whether HPV16 E6E7 and HRAS with or without exogenous MYC could confer tumor formation properties on other human cell types, including HBEC and HFF immortalized with hTERT (Figure 1D and E). Although, exogenous MYC expression resulted in the faster tumor-forming ability of HBEC ($P < 0.0005$), E6E7 and HRAS was sufficient for tumorigenic potential of these human cells with increased endogenous MYC levels (Figure 1C).

Then, we examined the effect of induced expression of MYC^{T58A}, which is a form resistant to FBWX7-dependent proteasomal degradation (9), on the tumorigenic potential of HCK1T-E with HRAS cells. Although MYC^{T58A} accumulation was observed in doxycyclin-treated cells both *in vitro* and *in vivo*, it did not result in increased tumorigenic potential in this setting (Supplementary Figure 1 is available at *Carcinogenesis* Online), indicating the possibility that certain threshold levels of MYC stabilized by HRAS might be sufficient.

Table 1. Summary of xenograft transplantation of HCKs

(A) Tumor formation using E6E7 expressing HCKs with HRAS^{G12V}

Cells	No. of tumors per sites of injection 1 × 10^6 cells per site	Weight of tumors (mg) at the end of the experiment (weeks)
HCK1T	4/4	460 ± 137 (3 weeks)
HCK1Ta	4/4	640 ± 479 (2 weeks)
HCK1Tb	4/4	500 ± 338 (2 weeks)
HCK1Tc	4/4	140 ± 50 (2 weeks)
HCK4T	4/4	523 ± 148 (2 weeks)
HCK4	4/4	225 ± 50 (3 weeks)
HCK8	4/4	555 ± 140 (3 weeks)

(B) Tumor formation using E6E7 expressing HCKs with HRAS^{G12V}

	2 × 10^3 cells per site (weeks)	2 × 10^2 cells per site (weeks)
HCK1T	6/6 (4)	6/6 (4)
HCK4T	4/4 (4)	4/4 (6)
HCK8T	4/4 (4)	4/4 (6)

(C) Tumor formation using E6E7 expressing HCK1T cells with MYC or other downstream signals of HRAS^{G12V}

	No. of tumors per sites of injection (1 × 10^6 cells per site)				
HCK1T-E6E7-	vect (weeks)	MYC	MYC^{T58A}	Tet-inducible-MYC^{T58A}	
				Dox+ (weeks)	Dox− (weeks)
Vect	0/7	0/4	0/4	0/3	0/3
BCL2			1/4	1/3	0/3
AKT	0/4			3/3 (9)	3/3 (9)[a]
MEK1DD	0/4			4/4 (7)	3/3 (7)[a]
HRAS^{G12V}	12/12 (2)			10/10 (6)[b]	10/10 (6)[b]

(B) Latency was determined as the time taken before a palpable mass could be detected and indicated in parentheses (weeks). (C) Incidence of tumor formation within 20 weeks of observation period was scored otherwise observation was terminated at the time indicated in parentheses (weeks). No description indicates not determined.

[a]Only small tumors developed as in Figure 3B and C.

[b]10^3 ($n = 4$) or 10^2 ($n = 6$) cells were transplanted.

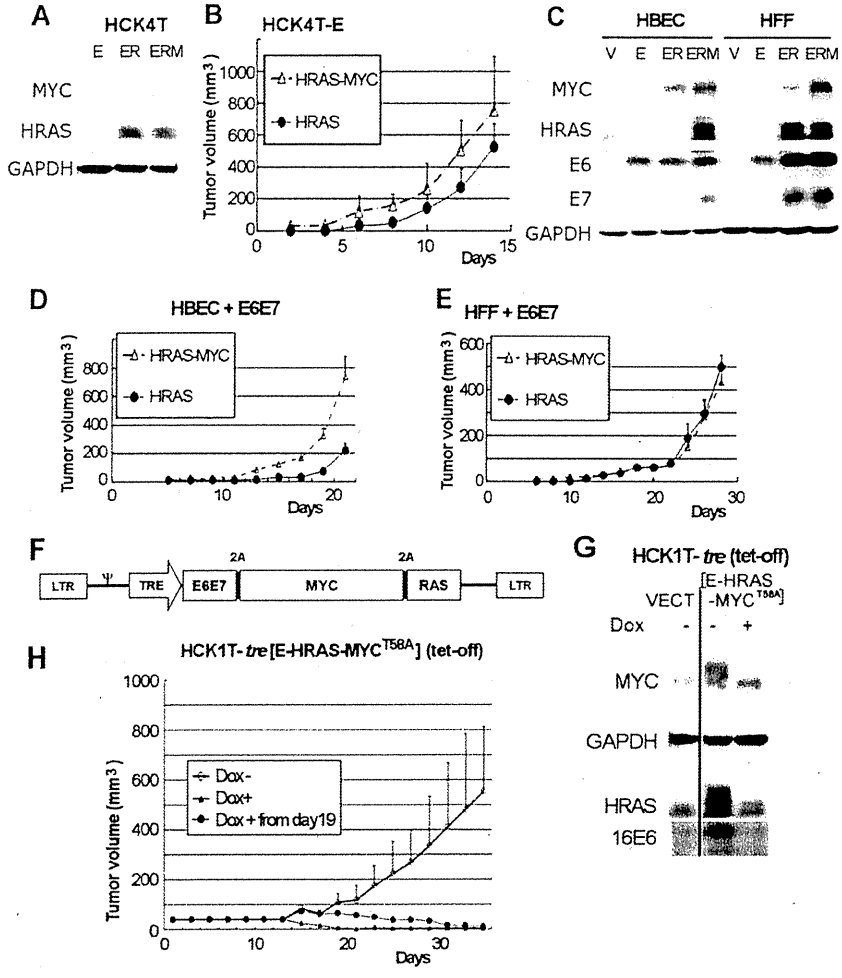

Fig. 1. HRAS with increased endogenous MYC expression is sufficient for full transformation of normal human cells expressing HPV16 E6E7. (**A**) Endogenous MYC levels in the presence of HRAS (ER) were compared with exogenous expression (ERM) by western blotting (ER for E6E7–HRAS and ERM for E6E7–HRAS–MYC). (**B**) *In vivo* tumor-forming ability of HCK4T-E cells with HRAS alone or HRAS–MYC. Cells were subcutaneously injected into nude mice (1×10^6 cells) and tumor size was measured every other day. The tumor volume (mm^3) was calculated as $L \times W^2 \times 0.52$, where L is the longest diameter and W is the shortest diameter. Each point is the mean of data for four to six samples ± SD. (**C**) Transgene products and MYC levels in human HBEC and HFF were determined by western blotting. (**D** and **E**) Tumorigenic ability of HBEC (D) and HFF (E) expressing HPV16 E6E7 and hTERT with HRAS alone or HRAS–MYC was determined as in (B). (**F**) Schematic of a single polycistronic virus in which expression of E6E7, MYC and HRAS are regulated by doxycyclin (Tet-off). These genes were separated by the sequences encoding the autonomous self-cleaving 2A peptides derived from foot-and-mouse disease virus (7). (**G**) The expression of the transgenes was determined by western blotting. (**H**) HCK1T cells transduced with this vector together with a Tet-off vector were transplanted into nude mice. When tumors had started to grow (the volume of the tumor exceeded 100 mm^3), the gene expression was terminated by adding doxycyclin in the drinking water.

To confirm that tumorigenicity is readily induced by expression of E6E7, HRAS and MYC (endogenous/exogenous) without further genetic changes and is reversible on cessation of such gene expression, E6E7, MYC^{T58A} and HRAS were cloned into a single lentiviral vector in which expression of transgenes was regulated by doxycyclin (Tet-off) (Figure 1F, G and H). HCK1T cells transduced with this vector together with a Tet-off (tTA) vector were transplanted into nude mice. When tumors had started to grow (the volume of the tumor exceeded 100 mm^3), the gene expression was terminated by adding doxycyclin to the drinking water and this resulted in halted tumor growth followed by complete regression (Figure 1H). These data support the idea that E6E7, HRAS and MYC are sufficient for tumor-forming ability of human cells without additional genetic alterations.

MYC stabilization by HRAS

We have reported that endogenous as well as exogenous MYC protein stability is increased in the presence of HRAS in exponentially growing HCK1T cells adapted to calcium and serum (grown in DMEM) (4). Because most of the data in this report were prepared with cells kept in KGM, which does not contain serum and high calcium, endogenous MYC protein stability was determined using HCK1T-E cells with a vector, AKT (myr-AKT1), MEK1DD [constitutively active form of MEK1which activates the extracellular signal-regulated kinase (ERK) pathway (10,11)] or HRAS in KGM. Endogenous MYC protein levels were increased in the order of the genes listed above (vector, AKT, MEK1DD and HRAS) (Figure 2A). In parallel with the MYC levels, Survivin (12), phosphorylated 4EBP1 (13) and phosphorylated p70S6K levels were increased and TSC2 levels were decreased (14). Increased ERK phosphorylation was observed in MEK1DD- and HRAS-expressing cells. Although similar trends were observed in subconfluent culture (data not shown), they were more evident under post-confluent culture conditions (Figure 2A).

Furthermore, increased MYC protein stability was found in the presence of HRAS (Figure 2C, also with post-confluent cells; data not shown) without significant increase in MYC messenger RNA

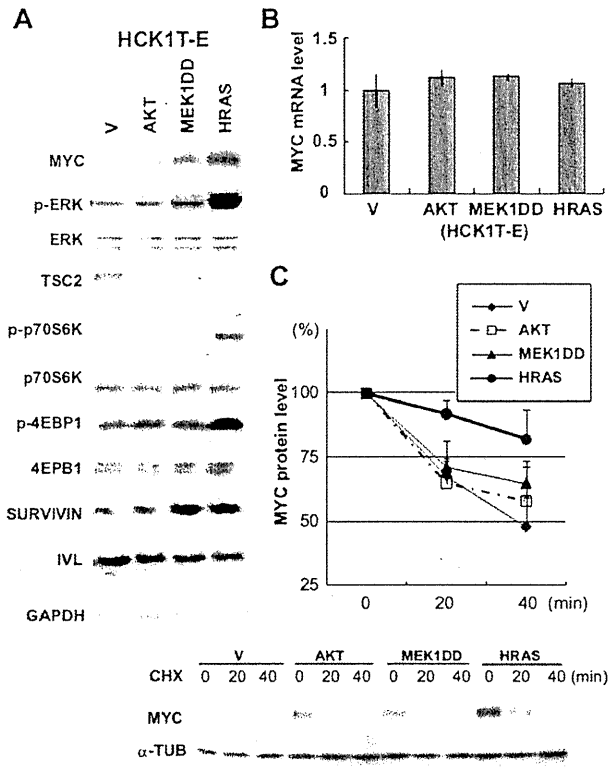

Fig. 2. Increased MYC protein stability in HRAS-positive cells.
(**A**) Endogenous MYC protein levels in HCK1T-E with vector, AKT (myr-AKT1), MEK1DD (constitutively active form of MEK1) and HRAS from post-confluent (3d) cells were determined by western blotting.
(**B**) Quantitative reverse transcription–PCR of MYC transcript levels from exponentially growing cells. Experiments were performed in triplicate and results were normalized to beta-2-microglobulin and presented as mean ± SD. (**C**) Exponentially growing cells were treated with 25 μg/ml cycloheximide (CHX) for the indicated time periods and the MYC degradation rate was assessed by western blotting. Results of quantitation in three experiments are shown with ± SD (**D**).

levels (Figure 2B). The levels of phosphorylated MYC, which has been reported to correlate with its function (15,16), were increased in the presence of HRAS (Supplementary Figure 2 is available at *Carcinogenesis* Online). From these observations, it is suggested that in HRAS-expressing cells, endogenous MYC expression is maintained at a higher level than in other cells.

Dissection of HRAS signaling pathways in tumor formation

In order to evaluate the importance of stabilized MYC for tumorigenic potential of HCK1T-E, we examined biological effects with MYC^{T58A}. Although we speculated that increased MYC expression is crucial for HRAS-induced tumorigenic potential, HCK1T-E with induction of MYC^{T58A} alone did not give rise to tumors. Though MYC^{T58A} mutant is reported to have reduced activity to induce apoptosis than MYC (16,17), it increased cleavage of caspase 3 in HCK1T-E cells (Figure 3A). To reduce the negative effect of MYC^{T58A}, BCL2 was introduced to HCK1T-E cells (Figure 3A). HCK1T-E with BCL2 cells showed weak tumor-forming ability upon MYC^{T58A} induction (Table I, C), but 4–5 months were necessary for palpable tumor masses, indicating a possible requirement for additional genetic and/or epigenetic alterations. MYC^{T58A} induction together with expression of either active AKT or MEK1DD conferred tumorigenic potential on HCK1T-E cells (Figure 3B and C). Although without induction of MYC^{T58A} they eventually started to form small tumors at the end of observation period (7–9 weeks), this might have been due to leakage of MYC^{T58A}

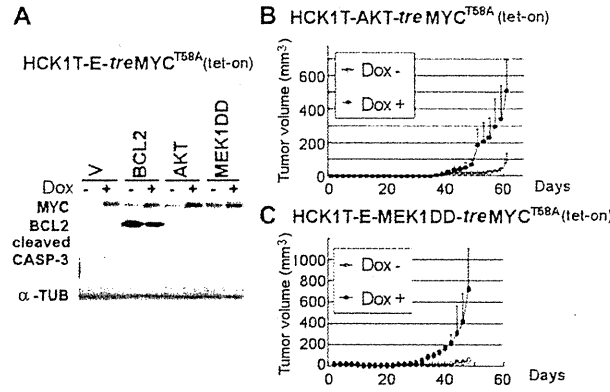

Fig. 3. Stabilized MYC expression is required for the tumorigenic potential of HCK1T-E cells with activated AKT or ERK. (**A**) MYC^{T58A} expression with the Tet-regulated expression system was determined by western blotting. Dox +; cells were treated with 1 μg/ml doxycycline (Dox) for 5 days. *In vivo* tumor-forming ability of AKT (**B**) and ERK (**C**) activated HCK1T-E cells with induction of MYC^{T58A} were determined as for Figure 1B. Mice were treated with doxycycline (1 μg/ml in their drinking water) or the vehicle (ethanol).

from the Tet-regulated expression system because HCK1T-E with AKT or MEK1DD alone did not form tumors within 20 weeks (Table I, C). Since tumorigenic potential was less than with HCK1T-E-RAS cells, it is evident that multiple RAS signaling pathways other than simply MYC stabilization are cooperatively involved in tumorigenic transformation of HCK1T-E cells.

MYC confers resistance to calcium- and serum-induced terminal differentiation and activates the mTOR pathway in HCK cells

Then, the biological effects of MYC on HCK were examined. Upon induction of MYC^{T58A} in HCK1T cells with BCL2, the expression levels of carbamoyl phosphate synthase/aspartate transcarbamoylase/dihydroorotase, a bona fide MYC target gene (18) and survivin (12) were increased, whereas the levels of a differentiation marker, involucrin, and a key inducer of keratinocyte differentiation, NOTCH1 (19), were decreased (Figure 4A). Furthermore, repression of TSC2 accompanied by activation of the mammalian target of rapamycin (mTOR) pathway was observed upon MYC^{T58A} induction. Activation of NOTCH1 and accumulation of involucrin induced by exposure to calcium and serum were largely canceled by MYC^{T58A} expression (Figure 4A). Similar effects of MYC^{T58A} induction were also observed in HCK1T-E cells with AKT or MEK1DD, although they were less marked, probably because E6E7 and AKT or MEK1DD influenced MYC regulation (17,20) (Figure 4B; data not shown). Induction of MYC^{T58A} significantly supported the growth of these cells in differentiating medium containing serum and high calcium, whereas no significant effects were observed in KGM (Figure 4C and D). Thus, MYC confers resistance to calcium- and serum-induced terminal differentiation and activates the mTOR pathway in HCK cells.

Inhibition of tumorigenic potentials of HCK1T-E–HRAS cells by inhibition of MYC or mTOR

Finally, we examined the role of endogenous MYC with HRAS in tumorigenic potential of HCK cells and cervical cancer cell lines (CaSki, SiHa, HeLa and C33A; Supplementary Figure 3B and C is available at *Carcinogenesis* Online; data not shown) by introducing the MYC inhibitor, OmoMYC (6), with Tet-regulated expression system, for which potential tumor-suppressive effects were recently reported in a mouse lung cancer model featuring KRAS mutation (21). OmoMYC induction levels were determined with an anti-MYC monoclonal antibody that recognizes both endogenous MYC and OmoMYC (Figure 5A). In contrast to the observations with MYC^{T58A} induction (Figure 4A and B), OmoMYC induction resulted

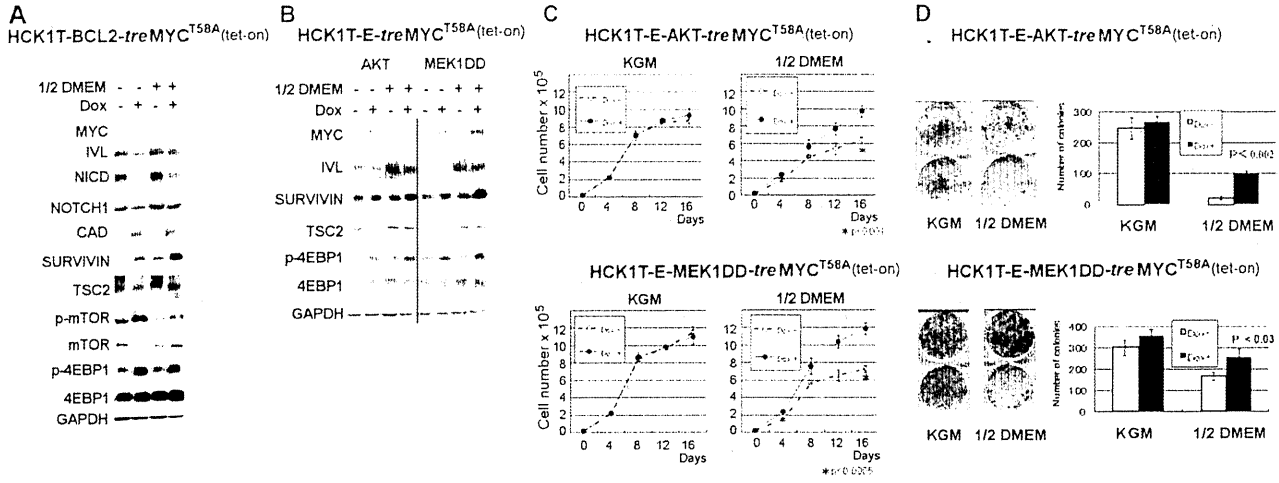

Fig. 4. Resistance to differentiation and mTOR activation by MYC. (**A**) HCK1T with BCL2 cells were treated with 1 μg/ml Dox for 3 days to induce MYC^{T58A} expression. Some cells were exposed to calcium and serum (KGM and DMEM were mixed at one to one ratio; 1/2 DMEM hereafter) for the last 1 day to induce calcium- and serum-induced terminal differentiation. Differentiation markers and MYC regulated genes were determined by western blotting. (**B**) HCK1T-E with AKT or MEK1DD with inducible MYC^{T58A} cells were treated as in (A). (**C**) Growth of cells in KGM (C left) and 1/2 DMEM (right, medium was replaced on day 1) were determined. A total of 2 × 10^4 cells were seeded on 22 mm dishes (BD Bioscience 3043) with the addition of Dox 1 μg/ml after 6 h and then counted on the indicated days. (**D**) The cells were seeded at a cell number of 2000 in wells of 35 mm dishes of six-well plates and 1 μg/ml Dox were added to the medium of three wells (dark bar) after confirmation of cell attachment (5 h). In half of the experiments, medium was replaced with 1/2 DMEM on day 2. After cultivation for 10 days, the cells were stained with Giemsa's dye, and the numbers of colonies were counted. Note that HCK1T-E with MEK1DD cells formed huge dense colonies with induction of MYC^{T58A} in clonogenic assay.

in increased involucrin and TSC2 (Figure 5A), further supporting regulation of these molecules through MYC in HCK cells. With induction of OmoMYC not exceeding endogenous MYC levels, HCK1T-E and HCK8T-E with HRAS cells did not result in significant reduction of growth (Figure 5B). Anchorage-independent growth ability of these cells was dramatically reduced with OmoMYC induction (Figure 5C) and tumorigenic potential was also profoundly reduced (Figure 5D). We obtained essentially the same result by moderate silencing of endogenous MYC in HCK1T-E with HRAS (Supplementary Figure 3A is available at *Carcinogenesis* Online). The induction of OmoMYC in cervical cancer cell lines also resulted in the suppression of their transforming abilities (Supplementary Figure 3B and C is available at *Carcinogenesis* Online). Although overexpression of MYC was not obvious in these cell lines, even in HeLa cells with a low level of MYC amplification (22), MYC might also play a critical role in these cells.

Because we found activation of the mTOR pathway in HRAS-transduced HCK cells, effects of an mTOR inhibitor, Rapamycin, on their transformation were tested. The clonogenicity of HCK1T-E with HRAS cells was reduced with Rapamycin in a dose-dependent manner (Figure 5E). Although either 10 nM Rapamycin or OmoMYC induction alone did not result in complete repression of clonogenic potential, simultaneous use of them blocked clonogenicity completely (Figure 5E), while strongly suppressing tumorigenic potential in nude mice (Figure 5F). These data indicate that the mTOR pathway is a major downstream effector activated by HRAS through MYC.

Discussion

MYC and RAS oncogenes can cooperatively induce full transformation of mouse cells but cause apoptosis and senescence, respectively, when expressed individually. Unlike the mouse cell case, transduction of MYC and RAS oncogenes into human cells does not suffice for full transformation, possibly because of more sophisticated tumor-suppressive failsafe mechanisms. However, we recently demonstrated that MYC and RAS can cooperatively transform human cells (HCKs) with the help of HPV16 E6 and E7 (4). In the development of cervical cancer, deregulated expression of E6 and E7 precedes disease progression, and E6 and E7 can immortalize HCKs and alleviate both MYC-induced apoptosis and RAS-induced senescence, mainly through inactivation of p53 and pRB. Here, we showed that oncogenic RAS on a background of E6E7 expression can induce full transformation of HCKs, and that stabilization of MYC by RAS is critical for tumorigenic transformation. Many mechanisms have been reported to be involved in MYC stabilization. A major ubiquitin ligase of MYC, FBXW7, preferentially recognizes and induces degradation of MYC with phosphorylated Thr58 and unphosphorylated Ser62, and thus the MYC^{T58A} mutant is very stable (23). Phosphorylation of Ser62 by ERK1/2 and inhibition of Thr58 phosphorylation through inactivation of GSK3β by AKT/PI3K are reported to be involved in RAS-induced MYC stabilization (17). Recently, CDK2 and downstream target(s) of PDK1 were also documented to phosphorylate Ser62 (24,25). Activities of these kinases can be regulated by multiple RAS signaling pathways as well.

If we could identify core gene sets, which promote reprogramming of normal human cells into cancer-generating cells, it would be of great advantage to understanding the complicated molecular mechanisms of carcinogenesis. In this study, we clarified that transduction of only three factors, namely oncogenic HRAS, E6 and E7, is sufficient for tumorigenic transformation of HCKs, though early studies have already suggested cooperation between E6E7 and oncogenic RAS (26–29). Thus, E6, E7 and HRAS might constitute one such core gene set. It also proved sufficient to induce full transformation of other normal human cell types, including human tongue keratinocytes, HBECs and HFFs though the HBECs and HFFs had been transduced with hTERT. Our recent study indicates that the role of E6E7 could be largely but not completely replaced by the blockade of the pRB and p53 pathways in human tongue keratinocytes (30). We previously found that ovarian surface epithelial cells could not be fully transformed by transduction of oncogenic KRAS and MYC with blockade of the pRB and p53 pathways by CDK4/CYCLIN D1 and a dominant-negative form of p53 (5). Other than inactivation of p53 and pRB, E6 and E7 proteins have many functions and it is very conceivable that these could be involved in full transformation. Indeed, in HCKs, the PDZ-binding motif of E6 is critical for full transformation of HCKs through degradation of several PDZ-containing proteins (our unpublished results).

Increased tumorigenic potential by exogenous MYC was observed with variation (Figure 1), indicating certain threshold levels of MYC are required for tumorigenicity depending on the cell type. However,

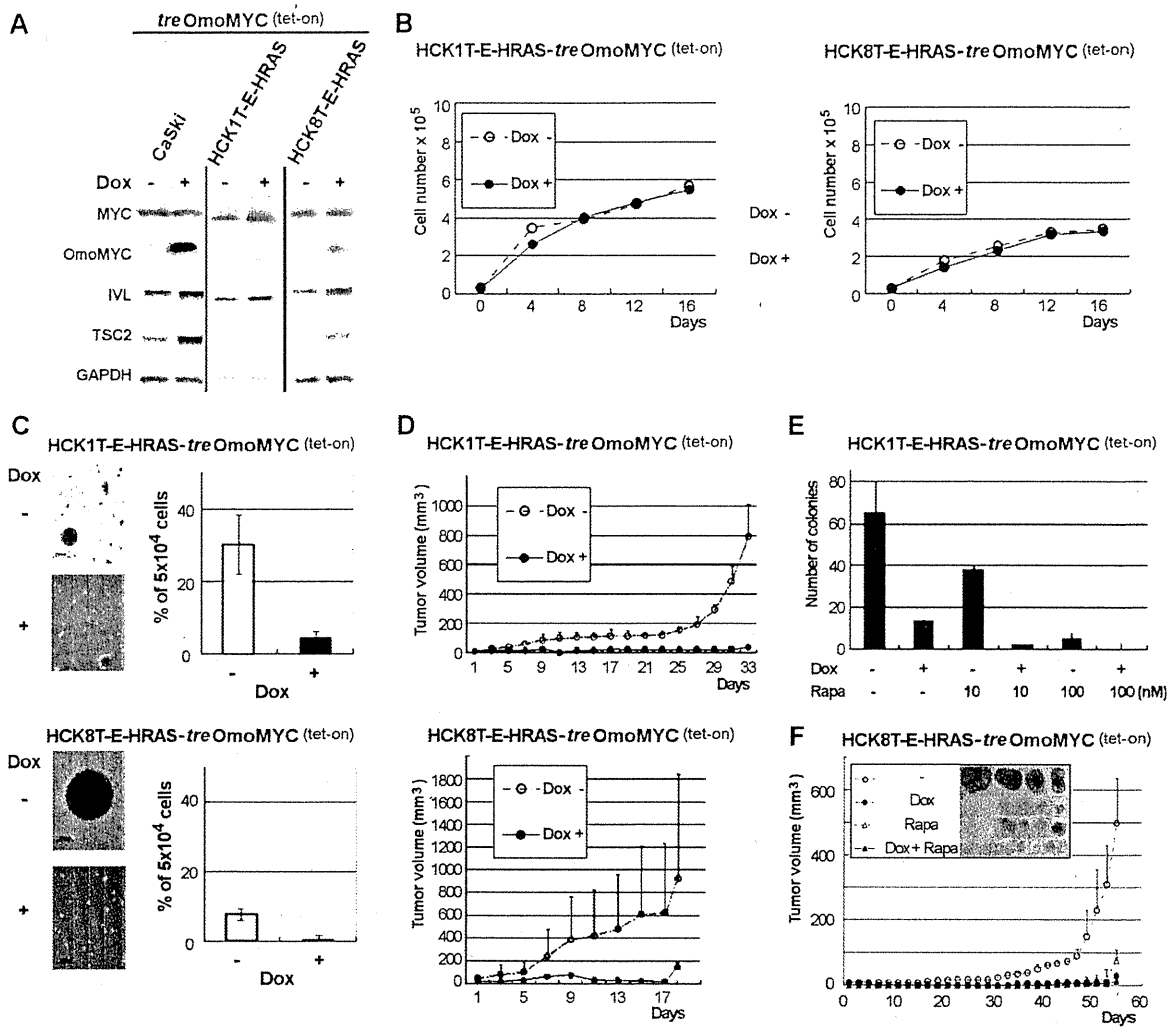

Fig. 5. Inhibition of MYC and/or mTOR pathway repressed tumorigenic potential of HCK cells with E6E7 and HRAS. (**A**) Induction of OmoMYC, an MYC inhibitor (Dox 1 μg/ml 5 days) and alteration of involucrin and TSC2 in HCK and CaSki cells were determined by western blotting. (**B**) Effects of OmoMYC induction on growth of HCK cells with E6E7 and HRAS were determined as for Figure 4C. (**C**) For assessment of anchorage independent growth of HCK cells with OmoMYC induction, aliquots (5×10^4 cells) were seeded in 35 mm dishes. After 3 weeks, the numbers of colonies (≥50 μm in diameter) were counted. (**D**) Effects of OmoMYC on tumor-forming ability of HCK cells were determined as for Figure 3B. (**E**) Clonogenic potential of HCK1T cells with OmoMYC or Rapamycin was determined as for Figure 4D. Indicated concentration of Rapamycin was added to the cells at day 1. (**F**) The effect of OmoMYC with Rapamycin on tumor-forming ability of HCK8T-E with HRAS cells was determined as in D. Mice were treated with 5 mg/kg Rapamycin administered by intraperitoneal injection twice a week.

transduction of four factors, E6, E7, RAS and MYC, proved sufficient for tumorigenic transformation of normal human cells tested here and broader cell types, including colon epithelial cells and pancreatic duct epithelial cells (data not shown), though hTERT might be additionally required for cells, such as HFFs, in which E6 cannot activate telomerase. In our previous study, HCK1T-E–HRAS–MYC cells adapted to DMEM showed much higher MYC expression than those kept in KGM (Supplementary Figure 4 is available at *Carcinogenesis* Online) with higher tumorigenicity, i.e. 10 DMEM-adapted cells formed huge tumors in ~50 days in contrast to the same cell number kept in KGM forming tiny tumors after ~100 days [(4) and data not shown]. DMEM-adapted cells might have gained the capacity to permit high levels of MYC and might give us a clue to understand further malignant conversion. Our preliminary data indicate that the DMEM-adapted cells exhibit epithelial–mesenchymal transition like changes, as determined by immunoblotting and microarray analysis (Supplementary Figure 4 and Supplementary Table 1 are available at *Carcinogenesis* Online).

We tried to dissect the RAS signaling pathways in order to define the critical factors for the promotion of cancer and found that activation of AKT or ERK pathway alone on the background of E6 and E7 expression was insufficient for full transformation. However, with additional induction of MYC^{T58A}, the cells acquired tumorigenicity in nude mice (Figure 3 and Table 1, C). These results allow us to hypothesize that one critical player to promote cancer 'stemness' downstream of HRAS signaling is elevated function of MYC. In normal HCK1T, induced expression of MYC^{T58A} inhibited terminal differentiation and increased expression of Survivin, which is implicated as a cancer stem cell marker (31) (Figure 4A). Furthermore, we found that TSC2 expression was repressed with induction of MYC^{T58A}, as reported recently for another cell type (14), accompanied by activation of the mTOR pathway.

It was recently reported that MYC sustains pluripotency of induced pluipotent stem and embryonic stem (ES) cells through repression of the primitive endoderm differentiation regulator, GATA6 (32), and our results indicate that MYC confers resistance to calcium- and

serum-induced terminal differentiation (Figure 4A–D) and the tumorigenic potential on non-tumorigenic HCKs (Figure 3). Although MYC-^{T58A} has reduced activity to induce apoptosis compared with wild-type MYC in the mammary gland (23), it does occur in a dose-dependent manner, even in the presence of E6 and E7 (Supplementary Figure 5 is available at *Carcinogenesis* Online) and remaining cells form tumors (Figure 3). We did not observe significant differences in the tumorigenic potential with the induction of MYC^{T58A} in HCK1T-E with HRAS cells (Supplementary Figure 1 is available at *Carcinogenesis* Online). It is also reported that low levels of deregulated MYC are competent to drive ectopic proliferation of somatic cells and oncogenesis, but overexpression of MYC wakes up the apoptotic and ARF/p53 intrinsic tumor surveillance pathways (33). These results clearly indicate that a certain threshold level of MYC is sufficient for tumor development, which is not affected by further overexpression, though such surplus expression of MYC might affect other pathological features such as metastasis.

MYC has been identified as one of four genes, which can reprogram fibroblasts into ES cells (34). Analysis of the ES cell-specific gene expression signature revealed that core pluripotency factors such as OCT4 and SOX2 are active in ES and induced pluipotent stem cells but not in cancer stem cells (35), but MYC regulatory networks are activated in both ES and cancer stem cells. Thus, MYC seems to play a role in normal ES cell biology and also cancer stem cells. MYC expression is deregulated in a wide range of human cancers and the rate of overexpression is generally more than the level of amplification (36). Cancers without amplification of MYC but with alterations in other oncogenes, such as RAS and growth factor receptors, which activate the function of MYC, could also be considered as MYC deregulated. Here, inhibition of endogenous MYC functions with Omo-MYC resulted in significant reduction of tumor formation and when the mTOR pathway activated by MYC was suppressed with Rapamycin, the tumorigenic potential of HCK cells was suppressed profoundly (Figure 5). To our knowledge, this is the simplest *in vitro* carcinogenesis model for human cancer and the first report indicating that endogenous MYC is a critical regulator of HRAS-induced tumor formation by human cells. The contribution of MYC to the cancer stemness might be broader than generally considered, and attempts to inhibit MYC functions with small molecules (37) as cancer therapy might be applicable to a wide range of malignancies.

Supplementary material

Supplementary Table 1 and Figures 1–5 can be found at http://carcin.oxfordjournals.org/.

Funding

This work was supported in part by a Grant-in-Aid for Cancer Research from the Ministry of Health, Labor and Welfare (10103828) and National Cancer Center Research and Development Fund (23-B1) to T.K., and a Grant-in-Aid for Scientific Research from the Ministry of Education, Culture, Sports, Science and Technology of Japan (21590452, 23300345) to M.N.-S. and T.K.

Acknowledgements

We thank Dr Kanai and Dr Ojima, Division of Molecular Pathology and the members of the Department of Gynecology for normal HCKs and would like to express our appreciation to Ms. Ishiyama for her expert technical assistance. We are grateful to Hiroyuki Miyoshi (RIKEN, BioResource Center) for CSII-EF-MCS and the related constructs.

Conflict of Interest Statement: None declared.

References

1. Walboomers,J.M. *et al.* (1999) Human papillomavirus is a necessary cause of invasive cervical cancer worldwide. *J. Pathol.*, **189**, 12–19.
2. zur Hausen,H. (2002) Papillomaviruses and cancer: from basic studies to clinical application. *Nat. Rev. Cancer*, **2**, 342–350.
3. Klaes,R. *et al.* (1999) Detection of high-risk cervical intraepithelial neoplasia and cervical cancer by amplification of transcripts derived from integrated papillomavirus oncogenes. *Cancer Res.*, **59**, 6132–6136.
4. Narisawa-Saito,M. *et al.* (2008) An *in vitro* multistep carcinogenesis model for human cervical cancer. *Cancer Res.*, **68**, 5699–5705.
5. Sasaki,R. *et al.* (2009) Oncogenic transformation of human ovarian surface epithelial cells with defined cellular oncogenes. *Carcinogenesis*, **30**, 423–431.
6. Soucek,L. *et al.* (2002) Omomyc, a potential Myc dominant negative, enhances Myc-induced apoptosis. *Cancer Res.*, **62**, 3507–3510.
7. Carey,B.W. *et al.* (2009) Reprogramming of murine and human somatic cells using a single polycistronic vector. *Proc. Natl Acad. Sci. USA*, **106**, 157–162.
8. Handa,K. *et al.* (2007) E6AP-dependent degradation of DLG4/PSD95 by high-risk human papillomavirus type 18 E6 protein. *J. Virol.*, **81**, 1379–1389.
9. Yada,M. *et al.* (2004) Phosphorylation-dependent degradation of c-Myc is mediated by the F-box protein Fbw7. *EMBO J.*, **23**, 2116–2125.
10. Brunet,A. *et al.* (1994) Constitutively active mutants of MAP kinase kinase (MEK1) induce growth factor-relaxation and oncogenicity when expressed in fibroblasts. *Oncogene*, **9**, 3379–3387.
11. Pages,G. *et al.* (1994) Constitutive mutant and putative regulatory serine phosphorylation site of mammalian MAP kinase kinase (MEK1). *EMBO J.*, **13**, 3003–3010.
12. Cosgrave,N. *et al.* (2006) Growth factor-dependent regulation of survivin by c-myc in human breast cancer. *J. Mol. Endocrinol.*, **37**, 377–390.
13. Balakumaran,B.S. *et al.* (2009) MYC activity mitigates response to rapamycin in prostate cancer through eukaryotic initiation factor 4E-binding protein 1-mediated inhibition of autophagy. *Cancer Res.*, **69**, 7803–7810.
14. Schmidt,E.V. *et al.* (2009) Growth controls connect: interactions between c-myc and the tuberous sclerosis complex-mTOR pathway. *Cell Cycle*, **8**, 1344–1351.
15. Watnick,R.S. *et al.* (2003) Ras modulates Myc activity to repress thrombospondin-1 expression and increase tumor angiogenesis. *Cancer Cell*, **3**, 219–231.
16. Chang,D.W. *et al.* (2000) The c-Myc transactivation domain is a direct modulator of apoptotic versus proliferative signals. *Mol. Cell. Biol.*, **20**, 4309–4319.
17. Meyer,N. *et al.* (2008) Reflecting on 25 years with MYC. *Nat. Rev. Cancer*, **8**, 976–990.
18. Eberhardy,S.R. *et al.* (2000) Direct examination of histone acetylation on Myc target genes using chromatin immunoprecipitation. *J. Biol. Chem.*, **275**, 33798–33805.
19. Yugawa,T. *et al.* (2007) Regulation of Notch1 gene expression by p53 in epithelial cells. *Mol. Cell. Biol.*, **27**, 3732–3742.
20. Veldman,T. *et al.* (2003) Human papillomavirus E6 and Myc proteins associate *in vivo* and bind to and cooperatively activate the telomerase reverse transcriptase promoter. *Proc. Natl Acad. Sci. USA*, **100**, 8211–8216.
21. Soucek,L. *et al.* (2008) Modelling Myc inhibition as a cancer therapy. *Nature*, **455**, 679–683.
22. Peter,M. *et al.* (2006) MYC activation associated with the integration of HPV DNA at the MYC locus in genital tumors. *Oncogene*, **25**, 5985–5993.
23. Wang,X. *et al.* (2011) Phosphorylation regulates c-Myc's oncogenic activity in the mammary gland. *Cancer Res.*, **71**, 925–936.
24. Hydbring,P. *et al.* (2010) Phosphorylation by Cdk2 is required for Myc to repress Ras-induced senescence in cotransformation. *Proc. Natl Acad. Sci. USA*, **107**, 58–63.
25. Tan,J. *et al.* (2010) B55beta-associated PP2A complex controls PDK1-directed myc signaling and modulates rapamycin sensitivity in colorectal cancer. *Cancer Cell*, **18**, 459–471.
26. Bowden,P.E. *et al.* (1992) Down-regulation of keratin 14 gene expression after v-Ha-ras transfection of human papillomavirus-immortalized human cervical epithelial cells. *Cancer Res.*, **52**, 5865–5871.
27. DiPaolo,J.A. *et al.* (1989) Induction of human cervical squamous cell carcinoma by sequential transfection with human papillomavirus 16 DNA and viral Harvey ras. *Oncogene*, **4**, 395–399.
28. Durst,M. *et al.* (1989) Glucocorticoid-enhanced neoplastic transformation of human keratinocytes by human papillomavirus type 16 and an activated ras oncogene. *Virology*, **173**, 767–771.
29. Hodivala,K.J. *et al.* (1994) Integrin expression and function in HPV 16-immortalised human keratinocytes in the presence or absence of v-Ha-ras. Comparison with cervical intraepithelial neoplasia. *Oncogene*, **9**, 943–948.
30. Zushi,Y. *et al.* (2011) An *in vitro* multistep carcinogenesis model for both HPV-positive and -negative human oral squamous cell carcinomas. *Am. J. Cancer Res.*, **1**, 869–881.
31. Li,F. *et al.* (2010) Generation of a novel transgenic mouse model for bioluminescent monitoring of survivin gene activity *in vivo* at various

pathophysiological processes: survivin expression overlaps with stem cell markers. *Am. J. Pathol.*, **176**, 1629–1638.
32. Smith.K.N. *et al.* (2010) Myc represses primitive endoderm differentiation in pluripotent stem cells. *Cell Stem Cell*, **7**, 343–354.
33. Murphy.D.J. *et al.* (2008) Distinct thresholds govern Myc's biological output *in vivo*. *Cancer Cell*, **14**, 447–457.
34. Takahashi.K. *et al.* (2006) Induction of pluripotent stem cells from mouse embryonic and adult fibroblast cultures by defined factors. *Cell*, **126**, 663–676.
35. Kim.J. *et al.* (2010) Myc network accounts for similarities between embryonic stem and cancer cell transcription programs. *Cell*, **143**, 313–324.
36. Vita.M. *et al.* (2006) The Myc oncoprotein as a therapeutic target for human cancer. *Semin. Cancer Biol.*, **16**, 318–330.
37. Shi.J. *et al.* (2009) Small molecule inhibitors of Myc/Max dimerization and Myc-induced cell transformation. *Bioorg. Med. Chem. Lett.*, **19**, 6038–6041.

Received July 14, 2011; revised January 19, 2012; accepted February 12, 2012

British Journal of Cancer (2012), 1–9

www.bjcancer.com

Full Paper

Creation of immortalised epithelial cells from ovarian endometrioma

Y Bono[1], S Kyo*[,1], M Takakura[1], Y Maida[1], Y Mizumoto[1], M Nakamura[1], K Nomura[1], T Kiyono[2] and M Inoue[1]

[1]Department of Obstetrics and Gynecology, Kanazawa University Graduate School of Medical Science, 13-1 Takaramachi, Kanazawa, Ishikawa 920-8641, Japan; [2]Virology Division, National Cancer Research Institute, 5-1-1, Tsukiji, Chuo-ku, Tokyo 104-0045, Japan

BACKGROUND: Epithelial cells of endometriotic tissues are difficult to propagate *in vitro* as experimental material is scarce owing to their limited life span. However, there is an increasing concern regarding their malignant transformation in ovaries. The present study sought to generate their stable culture system.

METHODS AND RESULTS: Purified epithelial cells isolated from ovarian endometriomas using microscopic manipulation were successfully immortalised by combinatorial transfection of human *cyclinD1*, *cdk4* and human telomerase reverse transcriptase (*hTERT*) genes, whereas the introduction of *hTERT* alone, or together with *cdk4*, was insufficient for immortalisation, leading to cellular senescence. We confirmed stable cytokeratin expression in the immortalised cells, proving their epithelial origin. These cells expressed progesterone receptor B and showed significant growth inhibition by various progestins. Oestrogen receptor (ER) expression was detected in these cells, albeit at low levels. Additional overexpression of ERα generated stable cells with oestrogen-dependent growth activation. Soft-agar colony formation assay and nude mice xenograft experiments demonstrated that these cells, even those with additional inactivation of *p53*, did not have transformed phenotypes.

CONCLUSION: We for the first time generated immortalised epithelial cells from ovarian endometrioma that retained sex steroid responsiveness. These cells are invaluable tools not only for the consistent *in vitro* work but also for the study of molecular pathogenesis or carcinogenesis of endometriosis.

British Journal of Cancer advance online publication, 21 February 2012; doi:10.1038/bjc.2012.26 www.bjcancer.com

Keywords: ovarian endometrioma; epithelial cells; immortalisation; progestin; oestrogen

Endometriosis is a common gynaecological disorder associated with dysmenorrhoea, pelvic pain and subfertility and is a leading cause of disability and loss of productivity in women of reproductive age (Olive and Schwartz, 1993). Numerous studies have attempted to dissect the biology of endometriosis. These studies mainly use *in vitro* culture of stromal cells rather than culture of epithelial cells from endometriotic tissues, because the former cells are more easily and stably cultured for much longer periods than the latter cells (Noble *et al*, 1997; Gurates *et al*, 2002). In fact, it is difficult to culture endometriotic epithelial cells *in vitro*, because these cells lose their proliferative capacity during ongoing cultivation of primary cultures over several days. The inability of endometriotic epithelial cells to survive *in vitro* is an obstacle to gaining a better understanding of the biology of this disease. In particular, malignant change of endometriosis, especially of ovarian endometrioma, for which epithelial cells are exclusively responsible, has lately attracted considerable clinical attention (Kurman and Craig, 1972; McMeekin *et al*, 1995; Ness, 2003; Oral *et al*, 2003). There is therefore an urgent need to establish a stable system for the culture of endometriotic epithelial cells that can be used for research not only into the biology of endometriosis but also into its carcinogenesis.

*Correspondence: Dr S Kyo; E-mail: satoruky@med.kanazawa-u.ac.jp
Received 12 September 2011; revised 28 November 2011; accepted 16 January 2012

There are two major barriers within epithelial cells that inhibit cell division under usual culture conditions: premature senescence and telomere-dependent senescence (Kiyono *et al*, 1998). The former is observed during early passage in primary culture and is caused by the activation of Rb that leads to cell cycle arrest, whereas the latter is found at a later stage of culture and is caused by telomere shortening after a considerable number of cell divisions. Inhibition of both Rb function and telomere shortening is therefore required for long-term culture of epithelial cells. In previous studies, we successfully established a stable system for the culture of primary endometrial epithelial cells, in which the human papillomavirus type 16 *E6/E7* genes and the human telomerase reverse transcriptase (*hTERT*) were introduced to inhibit Rb functions and to activate telomerase, respectively (Kyo *et al*, 2003). These immortal cells were not transformed but retained the original characteristics of endometrial epithelial cells, such as steroid responsiveness. Subsequent studies have demonstrated that overexpression of *cyclin D1* or *cdk4*, instead of HPV *E6/E7*, effectively inhibited Rb activity and might be an alternative method of overcoming premature senescence in primary epithelial cells of other origins (Ramirez *et al*, 2004; Sasaki *et al*, 2009).

In the present study, we sought to generate a stable culture of epithelial cells isolated from the ovarian endometriomas by the introduction of various genetic elements. These cells were successfully immortalised without generation of transformed phenotypes and were responsive to progestin and oestrogen.

These cells are thus potentially useful as an experimental model for analysis of the mechanisms of steroid hormone functions as well as of carcinogenesis arising from ovarian endometrioma.

MATERIALS AND METHODS

Isolation and purification of human endometriotic glands

Human endometriotic tissue samples were obtained from a 27-year-old and a 44-year-old patient undergoing laparoscopic ovarian cystectomy as a treatment for ovarian endometrioma with written informed consent. Briefly, tissues were gently minced into small pieces (1–2 mm^3) and were incubated for 1 h at 37 °C in a shaking water bath in 20 ml Hank's Balanced Salt Solution containing 0.2% collagenase type 3 (Washington Biochemical Corp., Lakewood, NJ, USA) and 1000 U of deoxyribonuclease I (Takara, Otsu, Japan). Epithelial glands were separated from stromal cells, blood cells and debris by serial filtration using narrow gauge sieves with apertures of 40–100 μm. Individual glands on the bottom of the dishes were directly picked up one by one under a microscope, collected into Eppendorf tubes and seeded onto 24-well dishes for subsequent gene transfection by viral vectors. The use of clinical materials obtained with written informed consent was approved by the Institutional Research Ethics Committee.

Vector construction and transfection

Viral construction and transfection of HPV16 *E6/E7* and *hTERT* have been previously reported (Kyo *et al*, 2003). Lentiviral vector plasmids were constructed by recombination using the Gateway system (Invitrogen, Carlsbad, CA, USA). Briefly, *hTERT*, *human cyclinD1* and *human mutant Cdk4* (Cdk4R24C: an inhibitor-resistant form of Cdk4 that was generously provided by Dr E Hara (The Cancer Institute of JFCR, Tokyo, Japan)) (Wölfel *et al*, 1995) were first recombined into entry vectors using the BP reaction (Invitrogen). These segments were then recombined with a lentiviral vector, CSII-CMV-RfA (a gift from Dr H Miyoshi (RIKEN BioResource Center, Tsukuba, Japan)) (Miyoshi *et al*, 1998), using the LR reaction (Invitrogen) to generate CSII-CMV-hTERT, -cyclinD1 and -hCDK4R24C. Production of recombinant lentiviruses with the vesicular stomatitis virus G glycoprotein was performed as described previously (Miyoshi *et al*, 1998). A dominant negative form of *p53* (*DN p53*) (Kiyono *et al*, 1994) was cloned into lentiviral vector plasmids by recombination using the Gateway system (Invitrogen). Oestrogen receptor α (ERα) overexpressing cells were established by lentiviral infection of the human ERα expression vector (pCMSCV-EM7bsd-hERα).

Cell culture

Stably established endometriotic epithelial cells were maintained in DMEM supplemented with 10% fetal bovine serum in an atmosphere of 5% CO_2 at 37 °C.

Reverse transcriptase–PCR (RT–PCR)

Total RNA was isolated from cells using the RNeasy Mini Kit (Qiagen Sciences, Germantown, MD, USA), and the first-strand cDNA was synthesised from 1 μg of total RNA by reverse transcription using Superscript II Reverse Transcriptase (Invitrogen) with random primers. Primer sequences and conditions for each gene are listed in Supplementary Table 1.

Western blot analysis

Nuclear extracts from cells were prepared using the method of Schreiber *et al* (1989). Subsequently, 50 μg of nuclear extracts were electrophoresed on a sodium dodecyl sulfate–polyacrylamide gel and transferred to polyvinylidene difluoride membranes. Membranes were blocked in TBST (150 mM NaCl, 20 mM Tris-Cl, pH 7.5 and 0.1% Tween) containing 5% nonfat dried milk and then incubated with specific antibodies against PR (H-190, dilution 1 : 1000, Santa Cruz Biotechnology, Santa Cruz, CA, USA) and actin (C-11, dilution 1 : 1000, Santa Cruz Biotechnology) followed by reaction with anti-rabbit IgG. Immunoreactive bands were visualised using the ECL detection system (GE Healthcare Biosciences, Pittsburgh, PA, USA), as suggested by the manufacturer.

Immunocytochemistry and immunohistochemistry

Cells were cultured on LAB TEK chamber slides (Nalge Nunc International, Naperville, IL, USA) for 24 h, fixed with methanol. For antigen retrieval of CD10, the sections were heated by boiling in 10 mM citrate buffer, pH 6.0 for 20 min followed by cooling at room temperature for 20 min. Slides were incubated for 60 min at room temperature with the following mouse monoclonal antibodies and working dilutions: anti-pan-cytokeratin (4/5/6/8/10/13/18) (C11, dilution 1 : 500, Santa Cruz Biotechnology) and anti-CD10 (clone 56C6, dilution 1 : 80, Leica Microsystems Inc., Buffalo Grove, IL, USA). After incubation with an anti-mouse secondary antibody, immune complexes were visualised using the ABC-elite kit (Vector Laboratories Inc., Burlingame, CA, USA).

β-gal assay

The β-gal assay was performed as previously described. Briefly, cells were fixed for 5 min at room temperature in 3% formaldehyde followed by incubation at 37 °C with senescence-associated β-gal stain solution containing 1 mg ml^{-1} of 5-bromo-4-chloro-3-indolyl β-D-galactoside (X-Gal), 40 mM citric acid/sodium phosphate, pH 6.0, 5 mM potassium ferrocyanide, 5 mM potassium ferricyanide, 150 mM NaCl and 2 mM $MgCl_2$. After 6–12 h incubation, positive staining was confirmed using microscopy.

In vitro growth assay

The proliferative activity of cells treated with progestins or oestrogen was examined by counting the cell number. Briefly, the cells were seeded at a density of 5–10 $\times$ 10^4 cells per well in six-well flat-bottomed plates and were grown overnight in normal growth media at 37 °C. Cells that had been pre-incubated in normal growth media or in phenol red-free media containing charcoal-treated fetal bovine serum for 24 h were treated with 17β-estradiol (E2), 6α-methyl-17α-hydroxy-progesterone acetate (MPA), progesterone or dienogest at various concentrations. Ethanol was used as a vehicle control.

Assay of aromatase activity

The aromatase activity of cells was assayed by detecting the formation of tritiated water from [1β-^{3}H]-androstenedione (PerkinElmer Genetics, Bridgeville, PA, USA) as described (Shozu *et al*, 1997). We used a 4-h incubation for the experiment. Aromatase activity was expressed as the rate of incorporation of tritium into water per milligram of protein per 4 h of incubation.

Anchorage-independent growth

A total of 2 $\times$ 10^5 Ishikawa cells or immortalised cells were seeded onto 6-cm dishes containing 0.33% Noble agar in DMEM supplemented with 10% fetal calf serum on top of a 0.5% agar base in DMEM supplemented with 10% fetal calf serum. Colonies >0.2 mm were counted after incubation for 2 weeks.